Retrofit of ship structural degradation

Davide Chichì

Thesis in partial fulfilment of the requirements for Master Degree in

Naval Architecture and Marine Engineering

Supervisor: Prof. Yordan Garbatov

Examination Committee

Chairman:	Prof. Carlos Guedes Soares
Supervisor:	Prof. Yordan Garbatov
Member of the Committee:	Prof. José Manuel Antunes Mendes Gordo

July 2017

Fear like limits are often just an illusion

M.J.

This page was intentionally left white

Acknowledgments

Many people showed their support during the entire course.

I want to thank my supervisor, Prof. Yordan Garbatov, for his motivation, availability, knowledge and exceptional guidance along the development of this study. It was a pleasure learning from him and working under his supervision.

To my girlfriend Arianne for her support and patience during those years.

To my family for their unlimited spirit and guidance during this period of my life.

To my brother and sister, that shared experience and wisdom.

To my curse colleagues Geordie and Federico for our shared experience through this course of study.

To my teammates of water polo, Club Oriental de Lisboa, for those two amazing year playing and training together.

To IST Lisboa for giving me this wonderful opportunity to enrich my knowledge.

A special thanks to my grandfather Quarto, passed away long ago, that inspired me and shared his great passion for the sea and ships

This page was intentionally left white

Abstract

The objective of the present study is to investigate the possibility to recover the ultimate strength of rectangular steel plate with a manhole shape opening subjected to uniaxial compressive load and randomized non uniform corrosion with the addition of stiffeners. A numerical experiment has been carried out to achieve the purpose. A total of four main models is created to perform finite element analysis with 63 sub-structured models. The non-uniform corrosion has been generated by Monte Carlo simulation with a presence of probability of 0% of pits.

The retrofitting process has been based on three scenarios: two longitudinal stiffeners, two longitudinal and two transverse stiffeners, the flange on the opening. The positioning of the stiffeners has been studied in three different locations. A preliminary study with an average uniform thickness of 8.5 mm has been carried out to determine the cases worth to study. A total of 10 cases has been selected and tested for the numerical experiment.

Three different assessments have been performed to evaluate the results: ultimate strength assessment, weight assessment and economical assessment. Two additional studies on effective thickness and plate slenderness have been carried out for a further comparison.

The study presented can be considered as a preliminary stage of a more complex method for prediction and solution of corroded plates with the installation of reinforcement.

Keywords: Plate with Opening; Corrosion; Ultimate Strength; Retrofit

This page was intentionally left white

Resumo

O objetivo do presente estudo é investigar a possibilidade de recuperar a resistência máxima da chapa de aço retangular com abertura de forma de passagem de homem sujeita a carga compressiva uniaxial e corrosão aleatória não uniforme com a adição de reforçadores. Um experimento numérico foi realizado para atingir o objetivo. Um total de quatro modelos principais são criados para realizar análise de elementos finitos com 63 modelos subestruturados. A corrosão não uniforme foi gerada pela simulação de Monte Carlo com uma presença de possibilidade de 0% de poritos de corrosão.

O processo de adaptação baseou-se em três cenários: dois reforços longitudinais, dois reforços longitudinais e dois transversais, flange na abertura. O posicionamento dos reforços foi estudado em três locais diferentes. Um estudo preliminar com uma espessura uniforme média de 8,5 mm foi realizado para determinar os casos que vale a pena estudar. Um total de 10 casos foi selecionado e testado para a experiência numérica.

Três avaliações diferentes foram realizadas para avaliar os resultados: avaliação final da força, avaliação do peso e avaliação econômica. Dois estudos adicionais sobre espessura efetiva e esbeltez da placa foram realizados para uma comparação adicional.

O estudo apresentado pode ser considerado um estágio preliminar de um método mais complexo de predição e solução de placas corroídas com a instalação de reforços.

Palavras-chave: Placa com Abertura; Corrosão; Tensão última; Retrofit

This page was intentionally left white

Contents

Table of Figures

List of Tables

This page was intentionally left white

List of Symbols

A_0	Sectional area plate
A_c	Compression cross sectional area
A_{plate}	Sectional area of the plate
$A_{c\ eff\ loc}$	Area of effective compression location
$A_{sl,l,eff}$	Effective cross-sectional area of the stiffener and the adjacent parts of the plate
A_{stiff}	Sectional area of stiffener
ASR	Average stress ratio
a, b	Parameter Garbatov (2007)
b, b_p	Breadth of plate
b_{eff}	Effective breadth
b_{ln}	Local breadth "n" of plate
β	Plate slenderness
C_0	Parameter for lateral shifting of the stiffener
d, D	Displacement
d_∞	Long-term corrosion wastage for plate
δ_{steel}	Density of steel
ε	Strain vector (Arch-Length)
E	Elasticity modulus
F^{int}	Internal forces
F^{ext}	External forces
h_w	Height of the stiffener web.
I	Second moment of Inertia
K	Stiffness matrix
K	Number of nodes
l	Length of plate
λ	Load vector
$\bar{\lambda}$	Relative column slenderness
m, n	Number of half waves
N	Axial load
ρ	Effective breadth parameter
R^i	Internal reaction forces
R^e	External reaction forces
$R_{y,i}$	Reaction forces in the *y*-direction at the i^{th} node
σ	Stress vector (Arc-Length)
σ_{max}	Maximum compressive stress
$\sigma_{cr\ c}$	Critical compression stress (unstiffened plate)
$\sigma_{cr\ l}$	Critical compression stress (stiffened plate)
σ_{YP}	Yield point of the material

t	Time in years
$t_{effective}$	Effective thickness
t_{stiff}	Thickness of the stiffener
t_p, z_0, h_0	Thickness plate
τ_c	Coating life
t_i	Average net thickness for intact or corroded plate
τ_t	Transition period
u	Displacement (Arc-Length)
ν	Poisson coefficient
V_{plate}	Volume of plate
V_{stiff}	Volume of stiffener
w_{Lmax}	Parameter for imperfections between stiffeners
w_{Gmax}	Parameter for imperfection between girders
$Z_{i,j}^{corroded}$	Randomized non uniform corroded plate
$Z_{i,j}^{corrosion\ depth}$	Random vertical reduction
$Z_{i,j}^{intact}$	Randomized thickness of the intact plate

1 Introduction

Marine structures are employed for carrying cargo, holidays, extracting natural resources located under the sea to the recent generation of electrical energy with offshore installations. The environment where they operate is harsh. The structures are subjected to corrosion, loads due the effect of sea waves, wind, machineries and cargo. All those factors cause solicitations to the structure during the service life. Marine structures themselves are composed of different elements: from frames to plates, all of them experience in different ways the environment and stresses.

A corroded plate loses the structural capacity to withstand loads and stresses. Marine structures spend almost the entire service life in water. Also, if those structures are protected against corrosion, it is a matter of time until corrosion starts. The protections are not perpetual; they have an effective time after which the corrosion process starts. It can be renewed, but it has a cost.

Classification Societies mark only the lower limit of the net thickness after which the structural element has to be substituted. In this period of economic crisis, it has become important to contain costs. A way to avoid the substitution of a part of the marine structure, it is to find a way to recover the initial capacity.

Classification Societies give this possibility with the substitution of material however they also accept a different approach. In particular, it has not been fully studied the possibility to recover the initial capacity with the addition of reinforced members to the aged panel. It is also important, from an economical point of view, to be able to predict when a structural element has to be reinforced, repaired or substituted.

The retrofitting process, intended as the process to recover the capacity of deteriorated structures, can become a reasonable synthesis between the containment of the cost, safety and prediction of the degradation of structures. It can also open a new flourish market for marine industries for not only repairs, but also preventive maintenance and protection of structures.

1.1 Motivation

Marine structures are composed of many different kinds of elements: plates, stiffeners, brackets and so on. One particular type of panel is widely used, but not fully studied. It is the plate with openings. To inspect marine structures, it is necessary to provide openings to pass from a local to another. Also to let pipes run along the whole structure, it is necessary to provide a way to pass through frames.

There are present studies about the capacity of this kind of panels to withstand stresses. A study that has not been carried out yet is about what happen when such structure is subject to corrosion. The corrosion process brings to a sensible loss of ultimate strength capacity. The fastest way to recover such capacity is to substitute partially or entirely the panel. A different approach has been thought to bring back such capacity and to prolong the service life of corroded panels with opening.

Corrosion has been investigated in different ways, with the creation of numerical models to predict the behaviour of such process on marine structures. Experiments have been carried out as well and recently, the application of

FEM analysis helped the study of aging structures. All those studies have been commissioned and investigated due to failures at sea of marine structures.

Different times such structures have failed also if they had met all the design criteria. Nowadays, more control and preventions has been done on structures to prevent excessive degradation or failure. This is highly connected to cost: the loss of a marine structure due to failure at sea is way greater than the repair cost. On the other hand, prevention has become the key factor to contain costs. Knowing when and how to repair an aged structure can make save a great amount of money.

FEM analysis, integrated with a corrosion simulator, can provide a reasonable estimation of the ultimate strength capacity of deteriorated plate and the value of such capacity of a renewed panel. Different solutions can be adopted and analysed by the FEM, giving a vast range of possibilities.

The main objective of this thesis is to model structural degradation of a plate with an opening and to provide a solution to recover the initial ultimate strength capacity with the addition of reinforced members to the corroded plate.

1.2 Aim and Scope

The present study aims to present a method for evaluating the retrofitting process of a panel with opening. In particular, a FEM analysis study has been conducted with structural and economical assessments. To predict the degradation of the panes, a Monte Carlo simulator has been used.

The thesis focuses the attention on the structural analysis of a steel plate with openings under uniaxial compressive load, with initial deformation and defined boundary conditions and the same steel panel with opening, under the same conditions, with different reinforced members. A total of four main different FEM models has been created to meet the conditions described previously. In addition to them, the sub-structuring of each model, brought in a total of 63 different FEM models to be tested.

The data collected from the FEM analysis permitted an evaluation of the different solution adopted for the retrofitting on strength, economy and weight level. This assessment can give the possibility to decide which solution might be more effective or rentable to adopt.

1.3 Thesis Structure

The thesis is structured as follows:

- Chapter 1: Introduction, Motivation, Aim and Scope, Thesis Structure;
- Chapter 2: State of Art, Theoretical Background
- Chapter 3: Finite Element Modelling
- Chapter 4: Retrofitting Assessment

- Chapter 5: Weight Assessment
- Chapter 6: Economical Assessment
- Chapter 7: Discussion, Final Remarks, Further Work

2 State of the Art

Numerous theoretical studies have been carried out on the determination of strength of corroded structures. The first step is to understand how corrosion act on an element and how time has a big influence on it. In many cases, corrosion has been considered variable linearly with the passing of time.

Linear corrosion wastage has been used principally in studies of reliability of structures such as Hart et al. (1986), Guedes Soares and Ivanov (1989).

From this point, studies were carried out considering multilinear models for the corrosion wastage: Southwell et al. (1979) presented a linear and bilinear model, Melchers (1998) a trilinear model while Yamamoto and Ikegami (1998) a three-stage model.

With Guedes Soares and Garbatov (1999), there is the theorization of a nonlinear model for the corrosion growth in three phases: durability of the coating, growth of corrosion and the progress of it. This model has been implemented and modified, but different authors: Sun and Bai (2001), Qin and Cui (2002), Paik et al. (2003), Ivanov et al. (2003).

An upload of the model of Guedes Soares and Garbatov (1999) was mad by Garbatov et al. (2005) with the implementation of experimental data from Wang et al. (2003).

Garbatov et al. (2014b), and Garbatov et al. (2016) described the effect of corrosion deterioration on corroded coupons subjected to tensile loading.

The principal element composing marine structures is a steel plate. Numerous studies have been conducted on the assessment of ultimate strength of steel panels.

The finite element method is a recent theory formulated in the early 1940s to solve complex structural analysis and elasticity problems in different branches of engineering. Collar and Duncan (1930-1935) introduced, for the first time, a primitive form of structural element in the resolution of the aero elasticity problem.

The finite element method is a recent theory formulated in the early 1940s to solve complex structural analysis and elasticity problems in different branches of engineering. Collar and Duncan (1930-1935) introduced, for the first time, a primitive form of structural element in the resolution of the aero elasticity problem.

Hrennikoff (1941) and Courant (1943) formulated the subdivision the domain problem in subdomains with the simplest form. Hrennikoff discretizes the domain by using a lattice analogy, Courant divided the domain into finite

triangular sub regions to solve second order elliptic partial differential equations from the problem of torsion of a cylinder.

In the middle of the 1950s, Turner formulated and perfected the Direct Stiffness Method, a first direct approach of finite element to the continuous field. This method had exclusive applicability in the aerospace engineering. Argyris and Clough applied the method of Turner to civil engineering. In particular, Argyris proposed a unification of flexibility method with direct stiffness method systematizing the concept of relations assemble of a structural system of relations of the component's elements. Clough was the first to introduce the Finite Element Method as it is known today.

In 1967 Zienkiewicz published the first book about the finite elements "The Finite Element Method in Structural and Continuum Mechanics" theorizing the application of finite element method in the study of structures.

Irons introduced the ISO-parametric elements, the concept of form, function, patch test, and frontal solver, an algorithm for linear algebraic system resolution.

Melosh framed the FEM method in the Rayleigh-Ritz method, class and systematized its variation formulation, later on improved by Strang, Fix and Wilson in 1973

In 1969 the Norwegian Classification Society Det Norske Veritas (DNV) developed the first software for FEM analysis of ships, SESAM.

Since the 1970s the FEM has been generalized and became a useful tool in different engineering fields.

Riks (1979) introduced the Arc-Length Method as a tool to solve complex non-linear equation with different critical points.

Several research studies have been conducted on the ultimate collapse capacity of plates and stiffened plates with an opening.

Shanmugam (1997) investigated the variation of ultimate strength in perforated thin plates and the incidence of the different positioning of the opening affecting the collapse strength.

Shanmugam et al. (1999), analysed the post buckling behaviour and the ultimate collapse strength of perforated plates under uniaxial or biaxial compression.

Paik et al. (2001) proposed formulae for the assessment of plates under the combination of biaxial compression and edge shear. This and other work of the same author were a prelude on an investigation of plates with opening.

Kim et al (2007) derived formulae for the assessment of ultimate strength in performed plate under axial compression. This study was implemented by a further formulation by Kim (2015) with experiments, both numerically and in scale, of perforated plates. In this study it has been proved the influence of different kind of stiffeners on the value of collapse strength.

Saad-Eldeen et al. (2013) derived a new expression for the assessment of ultimate strength of steel plates with large opening. The numerical experiment has been conducted comparing the result to the test conducted by Kim et al. (2009).

Saad-Eldeen et al. (2016) studied the influence of large openings on side shell plating demonstrating that the relation between the increase of the number of holes and the diminution of ultimate strength bending capacity is not linear.

Saad-Eldeen et al. (2016) conducted a series of numerical experiment for the assessment of the ultimate strength of plates with large openings.

2.1 Corrosion degradation

The corrosion of a material is a natural and irreversible process of slow and continuous consumption of the material itself and it results in the worsening of the physical characteristics or properties of the initial material. Metal corrosion can be defined as a process of degradation and re-composition with other elements in the environment: metals and alloys are at a higher energy level than the corresponding minerals, so under certain environmental conditions they tend to resume the most stable state present in nature, usually oxide, hydrate or salt. The most common type of corrosion is the electrochemical corrosion. Corrosion begins because in the metal there is a system that behaves like an electrochemical cell. On the surface of the artefact it has created an anodic zone in which the iron is oxidized:

$$anode\ (-)\quad Fe(s)\ \rightarrow\ Fe^{2+}(water) + 2\,e^{-} \tag{1}$$

The electrons move through the metal to another zone that acts as cathode where the reduction of oxygen in the presence of water happens:

$$cathode\ (+)\quad O_2\ (g) + 2H_2O\ (l) + 4e^{-}\ \rightarrow 4OH^{-}(water) \tag{2}$$

Fe^{2+} ions come into contact with ions OH^{-} and form a solid compound, poorly soluble in water:

$$Fe^{2+}(water) + 2OH^{-}(water)\ \rightarrow Fe(OH)_2\ (s) \tag{3}$$

Ferrous hydroxide in the presence of oxygen and water is then transformed into rust ($Fe_2O_3 * nH_2O$), a mixture of solid compounds containing ferric ions Fe^{3+} derived from the oxidation of ferrous ions Fe^{2+}.

The iron corrosion takes place more rapidly the greater is the electrical conductivity of the aqueous solution.

Corrosion can appear in different form and can be regrouped into the following categories (Dillon, 1982):

- Group 1: Identifiable by visual inspection
- Group 2: Identifiable with inspection tools
- Group 3: identifiable by microscopic examination

Marine structures are predominantly subjected to uniform corrosion and pitting corrosion. This study focuses the attention on the non-uniform corrosion of a steel plate.

2.2 Corrosion modelling

The corrosion deterioration modelling has different theorizations: linear, experimental and non-linear. The traditional approach is the linear modelling that considers corrosion grows linearly and brings to an overestimation of the deterioration. The experimental model is based on tests carried in determined conditions. That means that the model can be used only if the specific conditions are met in the finite element analysis which means that the applicability is limited. The non-linear model considers the corrosion depth as s non-linear time-dependent function of general corrosion wastage Silva et al., (2011).

The corrosion deterioration model used in the present study is the non-linear one theorized by Guedes Soares and Garbatov (1999). The present model considers the deterioration divided into three phases: in the first one there is no corrosion due to the coating protection of the plate, the second phase is the start of corrosion due to coating protection failure with a high corrosion rate, the third phase consists in the stop of the corrosion deterioration. The model is based on the solution of a differential equation of the corrosion wastage:

$$d_\infty(t) = \begin{cases} 0 & ,t < \tau_c \\ d_\infty \left[1 - exp\left\{-\frac{t-\tau_c}{\tau_t}\right\}\right] & ,t \geq \tau_c \end{cases} \quad (4)$$

Where τ_c is the coating life (time without corrosion), τ_t is the transition period, d_∞ is the long-term corrosion wastage for plater, t is the time in years. The three phases are described in Figure 1: the segment O'O indicates the first phase, OB for the second, after B for the third.

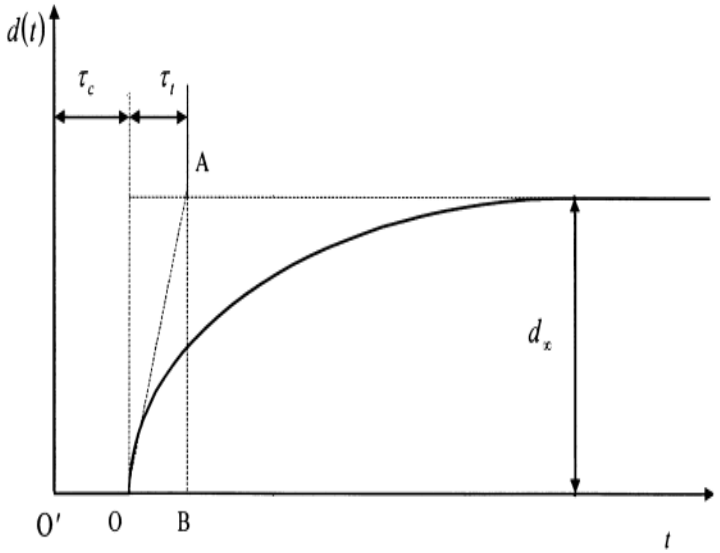

Figure 1 Time dependent corrosion model

The different parameters of the equation, valid for ballast tanks on tanker deck, are determined by Garbatov et al., (2007) as shown in Table 1.

Table 1 Parameters for ballast tanks of tanker beck, Garbatov et al., (2007)

$d_{\infty,ballast}$	1.85	[mm]
$\tau_{c,ballast}$	10.54	[years]
$\tau_{t,ballast}$	17.54	[years]

Further analysis was made by Garbatov and Guedes Soares, (2008) that demonstrates that the corrosion wastage depth can be described by Log-normal distribution.

$$StDev(t) = a\, Ln(t) - b \tag{5}$$

where the coefficients *a* and *b* are defined as 0.384 and 0.710 by Garbatov et al. (2007).

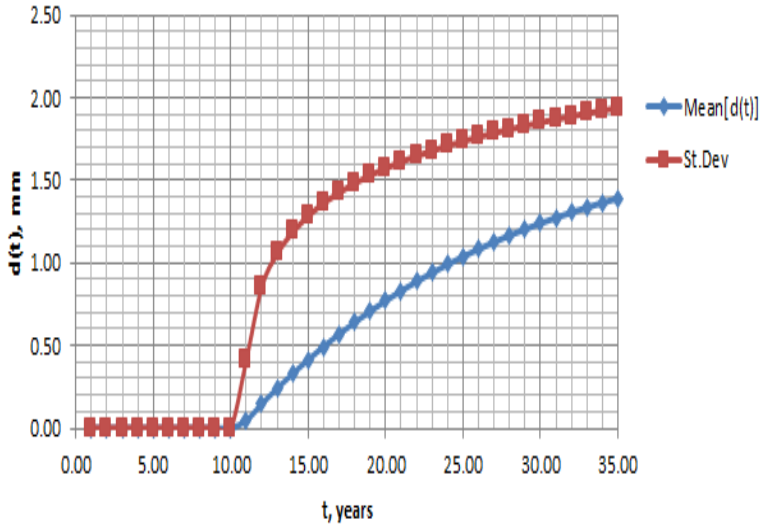

Figure 2 Mean and Standard deviation, Garbatov et al., (2007)

2.3 Monte Carlo Simulation of Corroded plate with opening

The non-uniformity of the corrosion degradation is given by the randomization of the plate thicknesses at each node by Monte Carlo simulation. Every node of the mesh used in the finite element analysis is described by x, y and z coordinates. For intact plate case, the z coordinate corresponds to the actual uniform thickness of the plate, 10 [mm] for this case study.

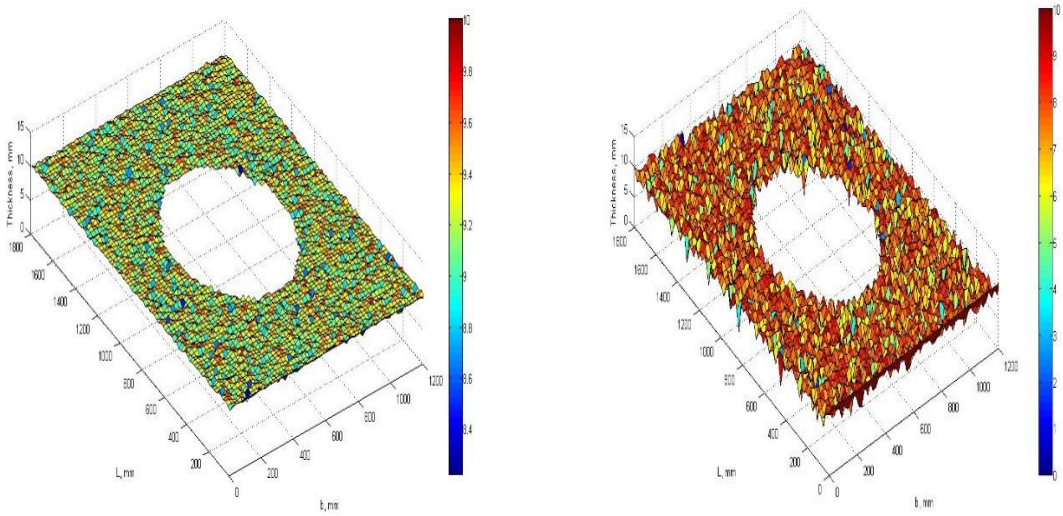

Figure 3 Modelled plate surfaces with an average thickness of 9.31 mm at 15th year (left) and 7.95 mm at 20th year (right)

The Monte Carlo simulator randomizes the intact thickness of which will be deducted the corrosion wastage depth in function of the year, Silva et al., (2011), as follow:

$$Z^{corroded} = Z^{intact} - Z^{\,corrosion\ depth} \tag{6}$$

Where $Z_{i,j}^{intact}$ is the randomized thickness of the intact plate with coordinates *x*, *y*, $Z_{i,j}^{corrosion\ depth}$ is the random vertical reduction and $Z_{i,j}^{corroded}$ is the randomized, non-uniform corroded plate.

The randomization of the two parameters, $Z_{i,j}^{intact}$ and $Z_{i,j}^{corroded}$ are applied to both panel and stiffeners with the exception of the edge $y = 0$ being the edge where is placed the node to assure symmetry and read the reaction forces.

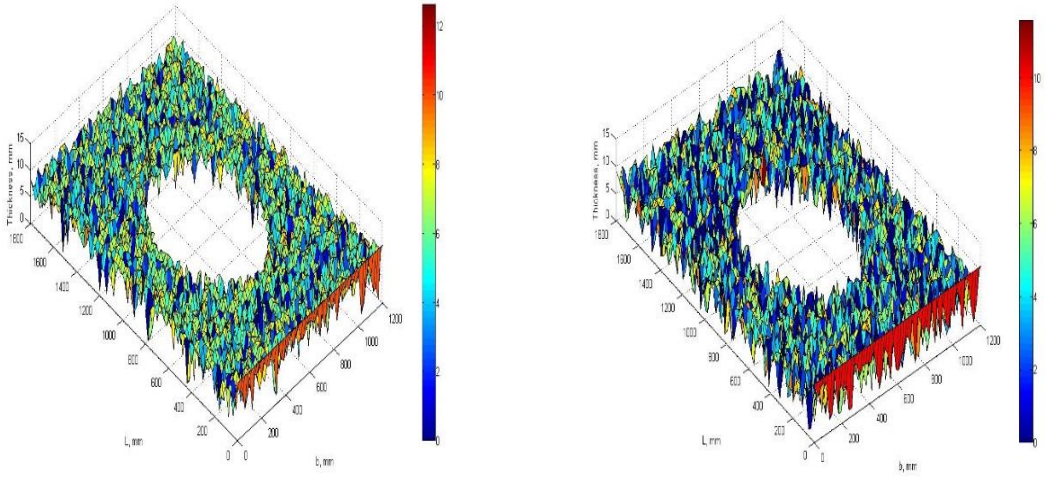

Figure 4 Modelled plate surfaces with an average thickness of 6.45 mm at 25th year (left) and 5.12 mm at 30th year (right)

Figure 5 shows the curves corresponding to the residual thickness of the plate and the corrosion wastage against the time. It is noticeable that after the transition time, τ_t, there is a reduction in the corrosion with an asymptotic behaviour of the curve towards the 40th years as demonstrated by Garbatov et al. (2007) with a consequent stabilization of the corrosion.

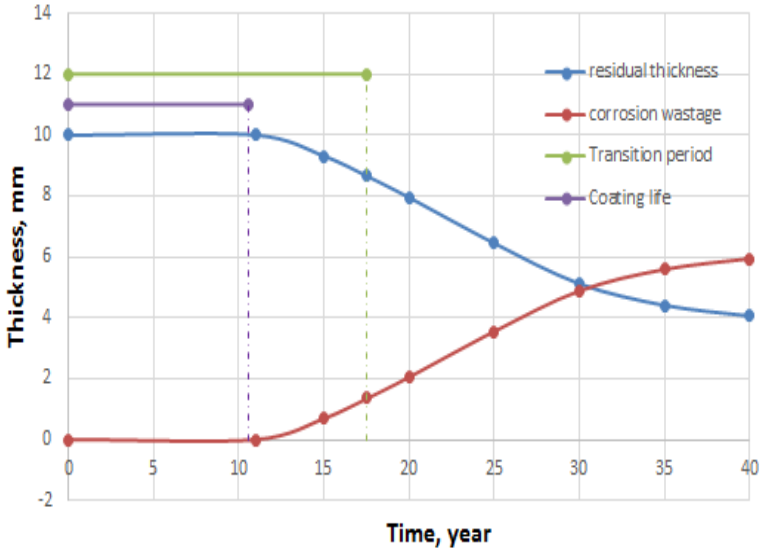

Figure 5 Time history of residual thickness and corrosion wastage of plate with opening

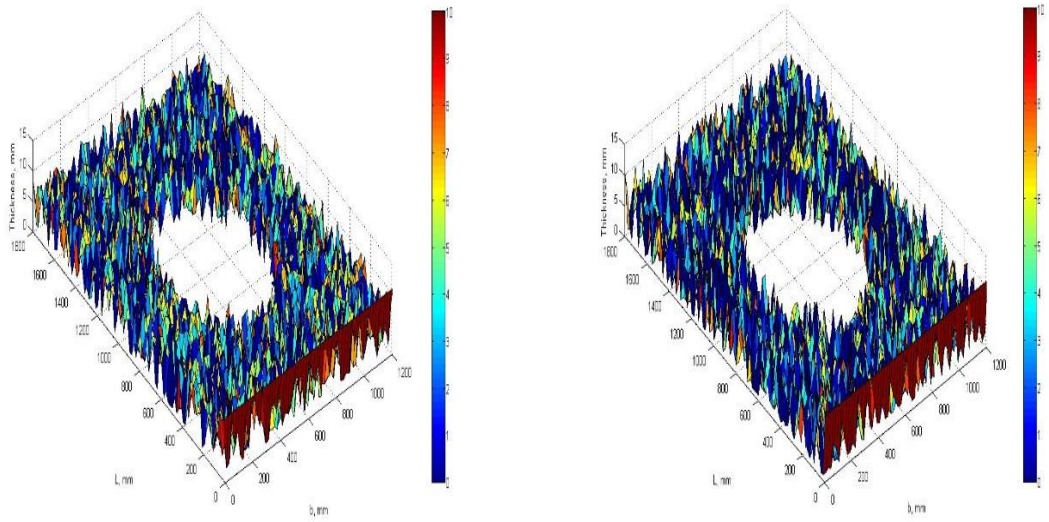

Figure 6 Modelled plate surfaces with an average thickness of 4.41 mm at 35th year (left) and 4.06 mm at 40th year (right)

2.4 Finite Element Method

The Finite Element Method permits to find a solution to complex problems (structural, heat transfer, etc.) by substituting with a simpler one. The solution obtained is an approximated one. Due the complexity of the system of equations generated to solve the original problem, in many cases, a direct approximated method does not exist. In those cases, the finite element analysis is preferred. FEM analysis can reach a reasonable approximated solution,

increasing the computational time and refining the sub-structuring of the model. Finite elements are defined as numerous, small and interconnected sub-regions of a body (Rao, 1982). The connections of the different elements are defined nodes and they are usually located on the element boundaries.

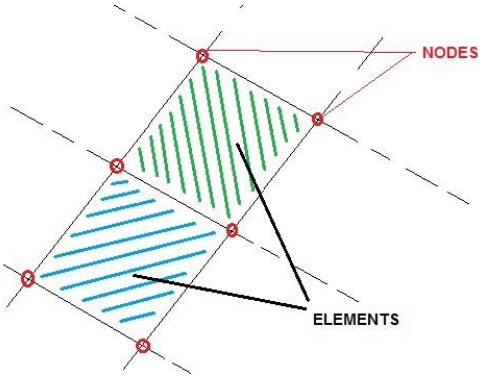

Figure 7 FEM nodes and elements

The main assumption in the FEM theory is that the variation of field variables in a finite element, such as displacement, stress, temperature, etc., can be approximated by a simple function. This assumption is done because the real variation of the field variables inside each element is unknown. Those functions, represented by interpolation models, are written in function of the field variables at each node. Once the equations of the entire field are determined, it remains to determine the nodal solutions. Those are given by solving the finite element equations, matrix equations. With the value of the field variable at each node determined, the interpolation methods approximate the field variable for the elements. This kind of analysis is called Linear. The non-linear analysis is used when the model presents non-linearity in geometry, material or contact.

The standard procedure for FEM analysis is composed of consequent steps from the description of the problem to the solution. The following list is a general guideline for the FEM Analysis proposed by Rao (1982) and Hutton (2003):

- Pre-processing
- Solution
- Post-processing

In the pre-processing, there are the definition of: geometric domain, element type, material properties of elements, geometric properties of elements, element connectivity, physical constraints, and loads.

In the solution process, the FEM software writes the matrix equations and calculates the unknown values of the field variables. The values obtained are then substituted to define additional variables as stresses, reaction forces, etc.

In the post processing all the values determined in the solution process are sorted, plotted and printed.

2.4.1 Linear and Non-Linear FEM Analysis

As exposed before, the main difference between linear and non-linear analysis is due the assumption done on the behaviour of material, geometric proprieties and contact. Taking into account the strain/stress curve of a material, the linear analysis covers only the first part, where the relation is proportional, as the figure shows. To obtain the remaining part of the curve, it is necessary to use the non-linear analysis due to the behaviour of such curve that presents non-linearity.

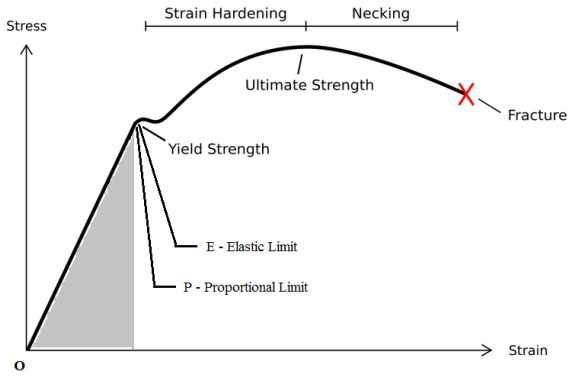

Figure 8 Stress-strain curve of steel

The grey region is the zone that can be covered by the linear analysis, for the remaining part it is necessary the non-linear one. This difference is reflected also in the formulation of the stiffness matrix.

The linear FEM analysis is based on:

Linearized geometrical equations, strain-displacement relations

$$\{\varepsilon\} = [B]\{d\} \tag{7}$$

Linearized constitutive equations, stress-strain relations

$$\{\sigma\} = [E]\{\varepsilon\} = [E][B]\{d\} \tag{8}$$

The equation of equilibrium

$$\{R^i\} = \{R^e\} \quad \rightarrow \quad [K]\{D\} = \{R^e\} \tag{9}$$

Suitable boundary conditions

In particular stiffness and forces are not functions of displacements:

$$[K]\{D\} = \{R\} \tag{10}$$

$$[K] \neq [K(\{D\})] \tag{11}$$

$$\{R\} \neq \{R(\{D\})\} \tag{12}$$

Non-linear behaviour occurs as stiffness and loads become functions of displacement or deformation:

$$[K]\{D\} = \{R\} \tag{13}$$

The structural stiffness matrix, $[K]$,and the load vector,$\{R\}$, become functions of the displacement,$\{D\}$. Therefore is not possible to solve the system for $\{D\}$ immediately as $[K]$ and $\{R\}$ are not known in advance. An iterative process is needed to obtain $\{D\}$ and the associated $[K]$ and $\{R\}$.

In particular stiffness and forces are functions of displacements:

$$[K]\{D\} = \{R\} \tag{14}$$

$$[K] = [K(\{D\})] \tag{15}$$

$$\{R\} = \{R(\{D\})\} \tag{16}$$

2.4.2 Solution strategies

There are three different approaches to solve a non-linear FEM analysis: increment of load (sub-steps), convergence iteration and a combination of the sub-steps and convergence criteria.

The increment of load consists in gradually raising up the applied load within a load step. The non-linear analysis depends on the load path followed. More sub-steps are provided for the analysis, smaller the increase of load is. This helps to improve accuracy and the easiness to converge.

The convergence iteration is based on the principle that within a load increment, an iterative method is used to find non-linear solutions. Nowadays there are different iterative methods used such as Newton-Raphson Method, Arc Length Method, Secant Method and many more. In this numerical study, it was used the Arc Length Method.

2.4.3 Arc-Length Method

The Arc-Length method is useful to solve non-linear system of equations when critical points arise in the formulation of the problem, for example when an instability occurs due to limited capacity of a loaded body to support an increase of external forces. This method uses two simultaneous variation of main parameters: displacement and load. The general equation of a non-linear system is given as follows:

$$F^{int}(u) - F^{ext} = 0 \implies F^{int}(u) - \lambda q = 0 \tag{17}$$

Supposing that the point (u_0, λ_0) satisfy the equation and being the variation of displacement Δu and the load vector Δλ, it can be written:

$$R(u', \lambda') = F^{int}(u_0 + \Delta u) - (\lambda_0 + \Delta\lambda)q = 0 \tag{18}$$

If the equation (18) is satisfied for$(u_0 + \Delta u, \lambda_0 + \Delta\lambda)$, also this point is on the equilibrium path and the solution can be updated. In the majority of simulations the immediate convergence to a solution is not possible, for this

reason the correction ($\delta u,\ \delta\lambda$) is taken into account with the target that the point ($u_0 + \Delta u + \delta u, \lambda_0 + \Delta\lambda + \delta\lambda$), will satisfy the equation(18). At this point it can be written:

$$R(u', \lambda') = F^{int}(u_0 + \Delta u + \delta u) - (\lambda_0 + \Delta\lambda + \delta\lambda)q = 0 \tag{19}$$

With the Taylor series expansion and keeping the linear terms, the previous equation can be written as:

$$F^{int}(u_0 + \Delta u) + \left[\frac{\partial F^{int}(u)}{\partial u}\right]_{u_0+\Delta u} * \delta u - (\lambda_0 + \Delta\lambda + \delta\lambda)q = 0 \tag{20}$$

where:

$$\left[\frac{\partial F^{int}(u)}{\partial u}\right] = [K_T] \tag{21}$$

The system of equations become:

$$[K_T]_{u_0+\Delta u} * \delta u - \delta\lambda q = -[F^{int}(u_0 + \Delta u) - (\lambda_0 + \Delta\lambda)q] = -R(u', \lambda') \tag{22}$$

When the *u* vector has dimension Nx1, there are N equations to be solved for N+1 undetermined parameter. The previous equation (22) cannot be used alone to determine $\delta u,\ \delta\lambda$. Another equation is introduced to complete the system:

$$(\Delta u + \delta u)^T * (\Delta u + \delta u) + \psi^2(\Delta\lambda + \delta\lambda)^2(q^T * q) = \Delta l^2 \tag{23}$$

where ψ and Δl defined by the user.

In general, the system of equations that has to be solved are:

$$\begin{bmatrix} [K_T] & -q \\ 2\Delta u^T & 2\psi^2\Delta\lambda(q^T * q) \end{bmatrix} * \begin{bmatrix} \delta u \\ \delta\lambda \end{bmatrix} = -\begin{bmatrix} R \\ A \end{bmatrix} \tag{24}$$

where:

$$R = F^{int}(u_0 + \Delta u) - (\lambda_0 + \Delta\lambda)q \tag{25}$$

$$A = -(\Delta u^T * \Delta u + \psi^2\Delta\lambda^2(q^T * q) - \Delta l^2) \tag{26}$$

The system of equations has to be solved for δu, δλ. The new corrections Δu and Δλ have become:

$$\Delta u' = \Delta u + \delta u \tag{27}$$

$$\Delta\lambda' = \Delta\lambda + \delta\lambda \tag{28}$$

The method keeps increment the correction δu, δλ until convergence is achieved. Figure 9 shows how such increments work.

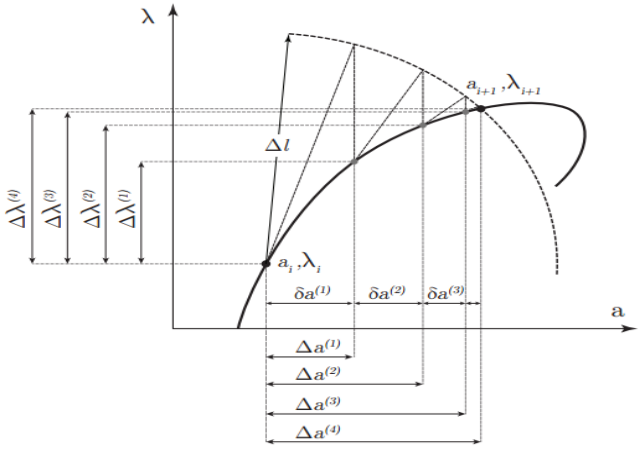

Figure 9 Graphic description of Arc-Length Method

2.4.4 Regimes of plate under compressive loads

Depending on the type of load the steel plate is experiencing, the regimes it passes through are different. When a steel panel is under predominant axial tensile loads, it fails by gross yielding, while when the steel plate is under predominant compressive loads (Paik at al., 2003), the regimes are:

- Pre-buckling
- Buckling
- Post-buckling
- Collapse (ultimate strength)
- Post-collapse

Figure 10 describes the regimes listed previously.

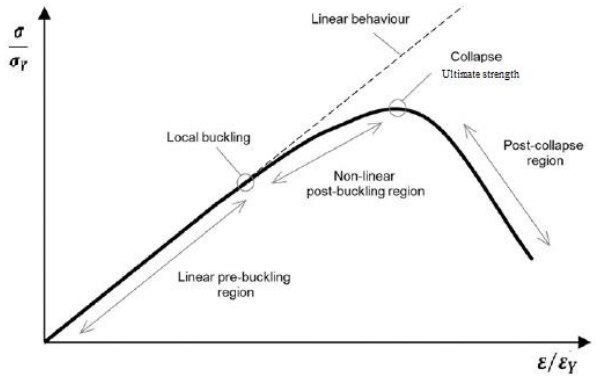

Figure 10 Regimes of plate under compressive load

The pre-buckling region presents a linear behavior between load and displacement. In this regime the structures are stable. The increase of compressive loads and the consequent reaching of critical values of them, cause the occurrence of buckling. It has to be remarked that for plates, buckling might happen in the elastic regime, but the structure can be considered stable, more loads can be sustained, until the ultimate strength also if the in-plane stiffness sensibly decreases after the commencement of buckling.

With the increasing of applied loads, the panel reaches the ultimate limit state cause by the increment of the yielded region. The post-collapse regime is characterized by high instability. The initial imperfection of a plate causes it to deflect at early stages with the increase of compressive loads. In this case the bifurcation buckling phenomenon does not appear (Paik, et al., 2003). As Figure 11 shows, the value of ultimate strength of imperfect structures is smaller than perfect structures.

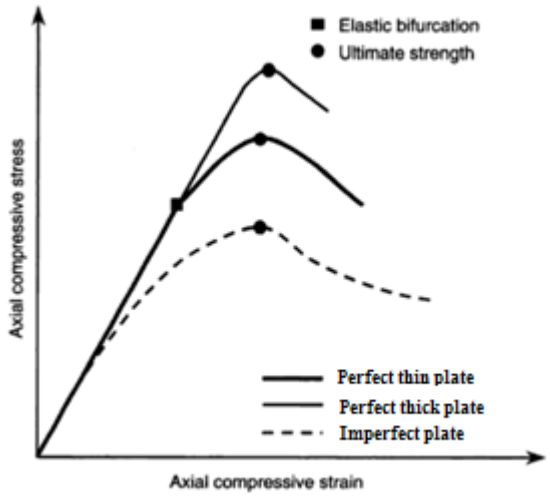

Figure 11 Ultimate strength and elastic bifurcation of perfect and imperfect plate

The ultimate strength of a plate is a function of different factors such as geometric and material proprieties, initial imperfections, boundary conditions, loading conditions, corrosion, cracks, dents, openings.

2.4.5 Slenderness Parameters

The plate subjected to uniaxial compression has a distribution of stresses that have a non-uniform behavior due to the increase of the compression when buckling occurs. In particular, such behavior happens because the central part of the plate has a higher tendency to buckle and the stresses on the edges increase while they decrease in the central zone. Figure 12 shows how the evolution of stresses occurs.

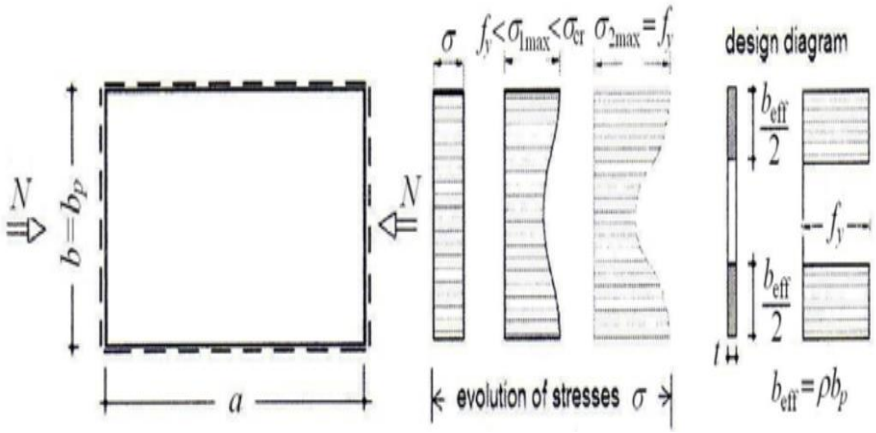

Figure 12 Evolution of stresses in plate under compression (Johansson *et al*., 2007)

The non-uniform distribution of stresses can be normalized with a uniform stress distribution that is a function of effective section. The EUROCODE 3 and the "Commentary and Worked Examples to EN 1993-1-5 „Plated

Structural Elements" furnish an indication to the approach to follow in the case of plate, stiffened or unstiffened, under compression.

The description of effective breadth b_{eff}, cross sectional area A_c and area of effective compression location $A_{c\,eff\,loc}$ are shown in Figure 13.

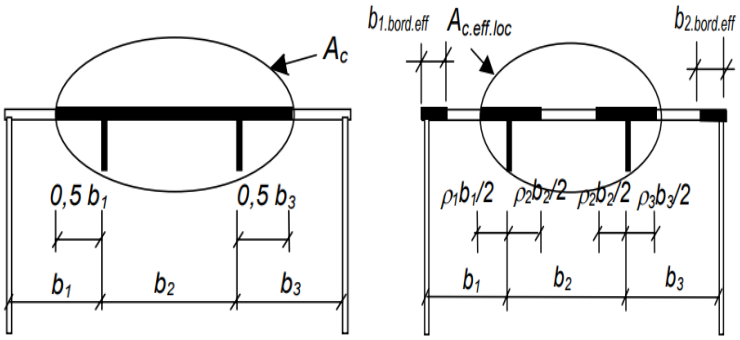

Figure 13 Definition of Ac (left) and Ac.eff.loc (right) for a stiffened plate element (uniform compression)

The critical compression stress for unstiffened plate is defined as:

$$\sigma_{cr\,c} = \frac{\pi^2 E\, t^2}{12(1-\upsilon^2)\, l^2} \tag{29}$$

As well the critical compression stress for stiffened plate is defined as:

$$\sigma_{cr\,l} = \frac{\pi^2 E\, I_{sl,l}}{A_{sl,l}\, l^2} \tag{30}$$

The relative column slenderness $\overline{\lambda}$ is defined as:

$$\overline{\lambda} = \sqrt{\frac{\sigma_y}{\sigma_{cr,c}}} \quad for\ unstiffened\ plate \tag{31}$$

$$\overline{\lambda} = \sqrt{\frac{\beta_{A,c}\sigma_y}{\sigma_{cr,c}}} \quad for\ stiffened\ plate \tag{32}$$

where

$$\beta_{A,c} = \frac{A_{sl,l,eff}}{A_{sl,l}} \tag{33}$$

$A_{sl,l,eff}$ is the effective cross-sectional area of the stiffener and the adjacent parts of the plate with due allowance for plate buckling (EUROCODE 3).

3 Finite Element Modelling

The plate considered for the study has a rectangular shape characterized by the following parameters: l is the length, b *is* the width and z_0 is the thickness. A manhole opening type, as shown in Figure 14, is present with a height of 800 mm and width of 400 mm. The elasticity modulus E considered for the study is equal to 205.8 GPa, the Poisson coefficient *v is* 0.3.

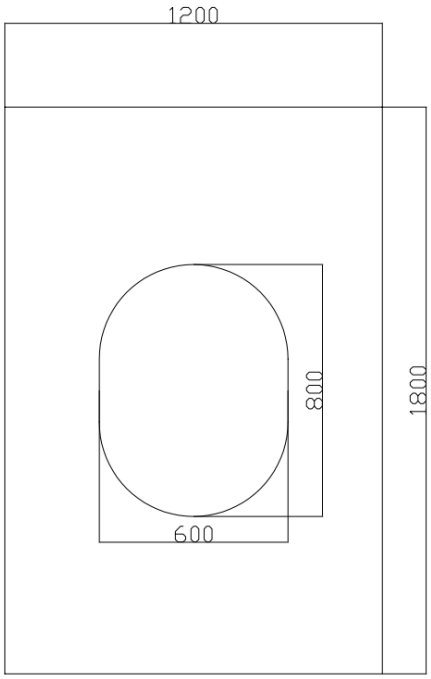

Figure 14 Geometry of plate with opening

The plate is oriented with the *z-axis* perpendicular to the plate, the *y-axis* aligned with the length l and the *x-axis* with the width *b*.

The study can be divided in two phases: first the analysis of the non-uniformed corroded plate with an opening, second the investigation of a proper solution to recover the ultimate strength capacity with the addition of stiffeners.

3.1 Boundary conditions

In all the cases analysed, the same boundary conditions were applied. The load applied to the panel is uniaxial, the displacement in the z-axis on all edges is not permitted, the rotations respectively in x-axis and y-axis direction are constrained at the edges $y = 0$ and $y = L$ for the first and $x = 0$ and $x = b$ for the second. The point with coordinates (b/2; 0; 0), called node1, is constrained to secure symmetry and to have an accurate determination of the displacement of the plate. The boundary conditions defined in this way are an accurate synthesis between the applicability of finite element analysis and the theory of simply supported panel. Table 2 presents the boundary conditions established for this study.

Table 2 Boundary conditions for FEM analysis

	U_x	U_y	U_z	Rot_x
y = 0	Free	Constrained	Constrained	Constrained
y = L	Free	Free	Constrained	Constrained
x = 0	Free	Free	Constrained	Free
x = b	Free	Free	Constrained	Free
node1	Constrained	Constrained	Constrained	Constrained

3.2 Initial imperfection

The initial global imperfection taken into account in this study is theorized by Faulkner (1975) as the maximum imperfections in a panel and it can be assumed proportional to β^2; it is also indicated the expressions to calculate the parameter for imperfections between stiffeners w_{Lmax} , the parameter for imperfection between girders w_{Gmax} and the parameter for lateral shifting of the stiffener C_0 as follows:

$$w_{Lmax} = a\, t_p \beta^2 \tag{34}$$

$$w_{Gmax} = 2\, mm \tag{35}$$

$$C_0 = 0.00323\, l \tag{36}$$

where β is the slenderness of the plate, t_p is the thickness of the plate, a is the coefficient to obtain the maximum local imperfection, in this case study is taken equal to 0.1, l is the length of the panel.

The plate slenderness β is defined as:

$$\beta = \frac{b}{t_p}\sqrt{\frac{\sigma_y}{E}} \tag{37}$$

where b is the width of the plate between stiffeners, t is the thickness of the panel, σ_y is the yield stress and E is the Young modulus.

For a simple rectangular plate and rectangular panel with opening, the global imperfection W_g is taken as following:

$$W_g = w_{gmax}\, sin\left(\frac{m\pi x}{l}\right) sin\left(\frac{n\pi y}{b}\right) \tag{38}$$

where l is the length of the plate, b is the breath of the plate, m and n are parameter depending on the number of waves considered, in this case the study is carried out for half wave ($m = n = 1$), $x \in [\,0, l\,]$ and $y \in [\,0, b\,]$.

In the cases with the addition of longitudinal stiffeners, it is necessary to take into consideration the contribution given by the local imperfection W_l. Figure 15 shows how the panel is divided into 3 different zone (A,B,C) having

for length the same length of the plate and for width 3 descriptive parameters $bl\ 1, bl\ 2, bl\ 3$ that vary in function of the positioning of the stiffeners.

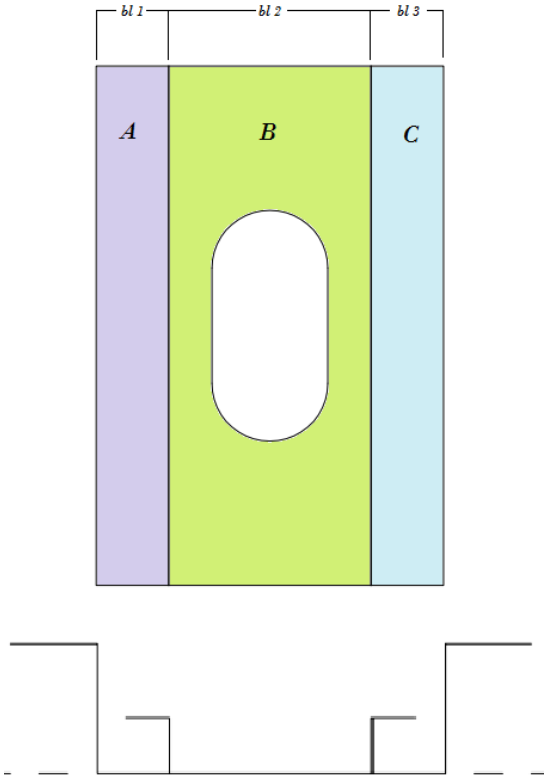

Figure 15 Plate with opening and two longitudinal stiffeners

The general equation describing the local imperfection between stiffeners is:

$$W_l = w_{lmax}\ sin\left(\frac{\pi m x}{l}\right)\ sin\left(\frac{\pi n y}{b}\right) \tag{39}$$

In the case of only two longitudinal stiffeners, the function become:

$$W_{l\ zone\ A} = w_{lmax}\ sin\left(\frac{\pi m x}{l}\right)\ sin\left(\frac{\pi n y}{b_{l1}}\right) \tag{40}$$

$$W_{l\ zone\ B} = w_{lmax}\ sin\left(\frac{\pi m x}{l}\right)\ sin\left(\frac{\pi n y}{b_{l2}}\right) \tag{41}$$

$$W_{l\ zone\ C} = w_{lmax}\ sin\left(\frac{\pi m x}{l}\right)\ sin\left(\frac{\pi n y}{b_{l3}}\right) \tag{42}$$

where b_{l1} is the local width between girder and stiffener (zone A), b_{l2} is the local width between two stiffeners (zone B) and b_{l3} is the local width between stiffener and girder (zone C). In all the cases it was assumed $b_{l1} = b_{l3}$.

The same approach was used for the case with two longitudinal and two transversal stiffeners as shown in Figure 16.

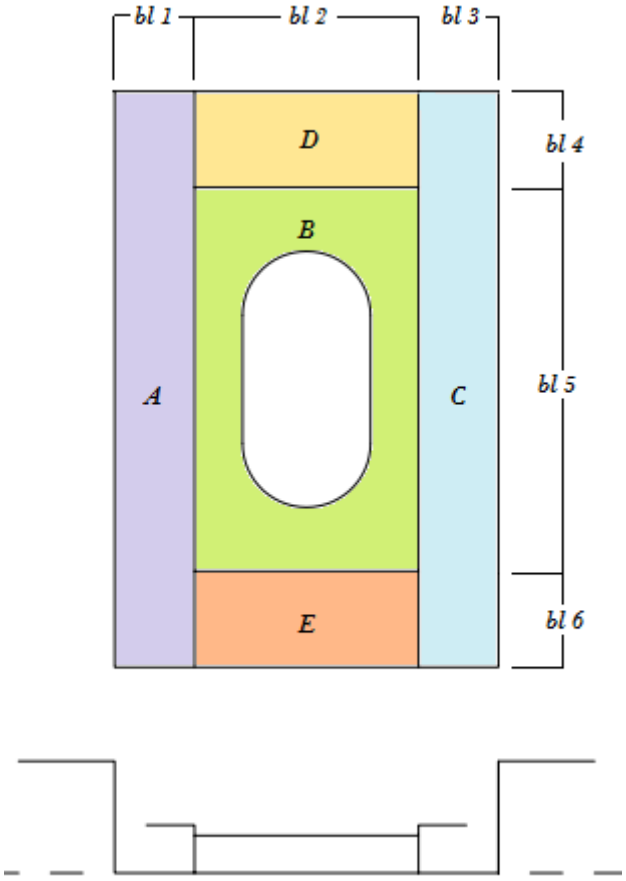

Figure 16 Plate with opening and two longitudinal and two transverse stiffeners

b_{l1}, b_{l2} and b_{l3} are defined as the previous case, b_{l4} as the local length between the edge of the plate and the transversal stiffener, b_{l5} as the local length between the two transversal stiffeners and b_{l6} as the local length between the second transverse stiffener and the edge of the plate.

$$W_{l\ zone\ D} = w_{lmax}\ sin\left(\frac{\pi m x}{b_{l4}}\right)\ sin\left(\frac{\pi n y}{b_{l2}}\right) \tag{43}$$

$$W_{l\ zone\ B} = w_{lmax}\ sin\left(\frac{\pi m x}{b_{l5}}\right)\ sin\left(\frac{\pi n y}{b_{l2}}\right) \tag{44}$$

$$W_{l\ zone\ E} = w_{lmax}\ sin\left(\frac{\pi m x}{b_{l6}}\right)\ sin\left(\frac{\pi n y}{b_{l2}}\right) \tag{45}$$

In all cases with this kind of configuration $b_{l1} = b_{l3}$ and $b_{l4} = b_{l6}$.

Particularity of this configuration is that in the central zone with the opening (zone B) the local imperfection is given by the

In the case with the flange, the only imperfection taken into account in the study is the global imperfection of the plate.

In all cases the lateral shifting of the stiffener is given by:

$$W_{stiff} = C_0 \frac{t_{stiff}}{h_w} sin\frac{\pi x}{l} \quad (46)$$

where t_{stiff} is the thickness of the stiffener, h_w is the height of the stiffener web.

Figure 17 shows the interaction of the three different initial imperfections acting on a plate with stiffeners.

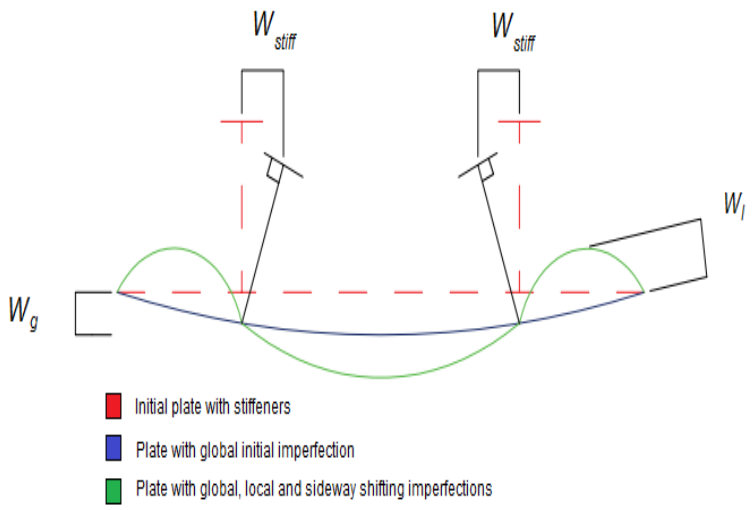

Figure 17 Global and local imperfection of plate and sideway shifting imperfection of stiffeners

3.3 Element size

The find the most convenient element size for the model that can give reasonable results with less time wastage as possible, a series of finite element analysis has been carried out for intact plate and intact plate with an opening. In particular, it was decided to use five different element sizes and to compare the results. The finite element analysis has been performed for the intact plate case and for the intact plate with an opening and the results were compared with numerical calculations.

3.4 Element type

In all cases the element type used in the analysis is shell element SHELL181. The element has four nodes with six degrees of freedom at each node: translations in the x, y, and z directions, and rotations about the x, y, and z-axes. SHELL181 is well-suited for linear, large rotation, and/or large strain nonlinear applications, change in shell thickness is accounted for in nonlinear analyses. In the element domain, both full and reduced integration schemes are supported (ANSYS 2016).

3.5 Convergence iteration

The convergence iteration method used in the numerical simulation is the Arc-Length. In particular, it was necessary to set the values of minimum arc length to 10^{-7} (default 10^{-3}) to get convergence in the solution process.

4 Stress-strain relationship

The stress-strain curve displays the relation between load and stress on a structural member or specimen of material and the corresponding strain or deformation. The analysis is carried out applying an axial load in the *y* direction on the edge $y = l$ while the reaction forces are calculated on the opposite edge $y = 0$. The averaged stress ratio *ASR* is defined as the sum of the reaction forces $R_{y,i}$ in the *y*-direction at the i^{th} node with coordinates $(x_i, 0,0)$, k is the number of nodes at $y = 0$, A_0 is the sectional area, σ_{YP} is the yield point of the material (Silva et al. 2011).

$$ASR = \frac{\sum_{i=1}^{k} R_{y,i}}{A_0 \sigma_{YP}} \tag{47}$$

The sectional area is defined as:

$$A_0 = b * t_i \quad for\ simple\ plate \tag{48}$$

$$A_0 = A_{plate} + A_{stiff} \quad for\ stiffened\ plate \tag{49}$$

where t_i is the average net thickness of an intact or corroded plate, A_{plate} is the sectional area of the plate calculated as $A_{plate} = b * t_i$, A_{stiff} is the sectional area of the stiffeners. The sectional areas are always calculated at the edge of reaction forces $y = 0$.

4.1 Intact plate

In the case of intact plate, the element sizes used are shown in Table 3.

Table 3 Intact plate element size and number of elements

case	element size [m]	number of elements
1	0.01	21901
2	0.015	9801
3	0.02	5551
4	0.025	3577
5	0.03	2501

The *ASR* curves as a function of the finite element size are shown in Figure 18.

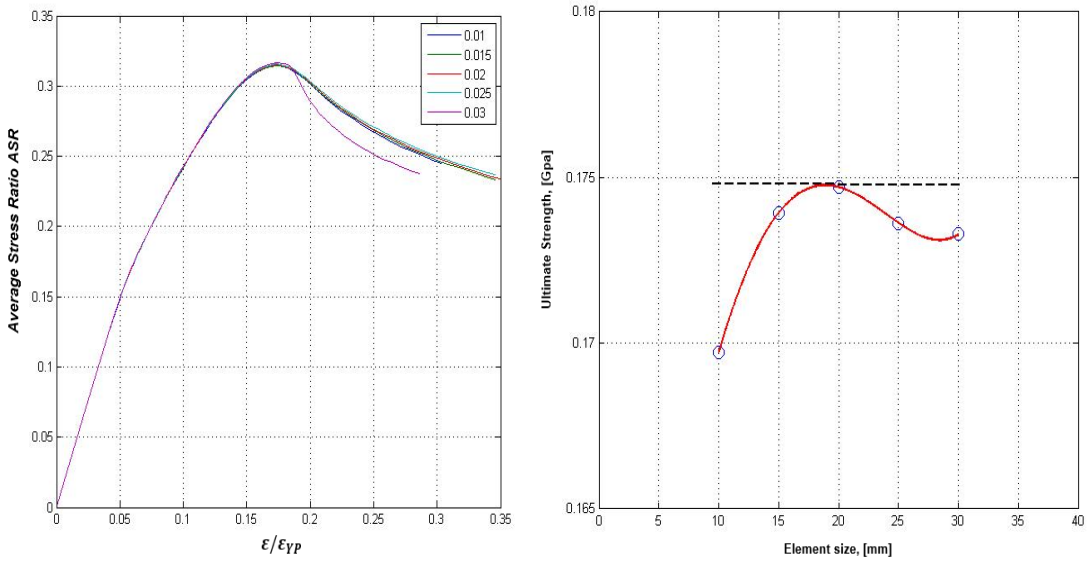

Figure 18 Stress-strain curves for different element sizes (left), Element size vs Ultimate Strength (right)

The gradient of the ultimate strength of the plate with respect to the element size is calculated with the formula indicated in "Ultimate strength assessment of steel plates with large openings" (Saad-Eldeen et al. 2014) as follows:

$$Gradient = \lim_{\Delta ES \to 0} \frac{\Delta \sigma_u(ES)}{\Delta ES} \cong \frac{\sigma_{u,i} - \sigma_{u,i+1}}{ES_i - ES_{i+1}} \tag{50}$$

The selected element size for all analyses of this study is 20.0 [mm]. This value gives the best fit for a number of elements and time occurred in the finite element analysis.

A different series of finite element analysis were carried out varying the plate thickness. This kind of analysis was useful to understand how the thickness affects the strength capacity of the plate to withstand loads. The figure below shows, for different thicknesses, the stress strain curve for intact plate.

4.1.1 Influence of variation of thickness

A series of analysis with different uniform thicknesses for intact plate were carried out to study the variation of the stress-strain curve at the changing of thickness. Table 4 shows the tests performed.

Table 4 Thicknesses tested to check influence of variation of thickness

Test n°	Thickness [mm]	Test n°	Thickness [mm]
1	6.0	6	11.0
2	7.0	7	12.0
3	8.0	8	13.0
4	9.0	9	14.0
5	10.0	10	15.0

The first figure shows how the decrease of the thickness affects the capacity of the panel to withstand loads and give a clear idea of how the corrosion, as well, reduces that capacity. The second figure describes the ultimate

strength ratio in function of the thickness. Also from Figure 19, it is possible to observe that the collapse strength varies linearly with the increase of panel thickness.

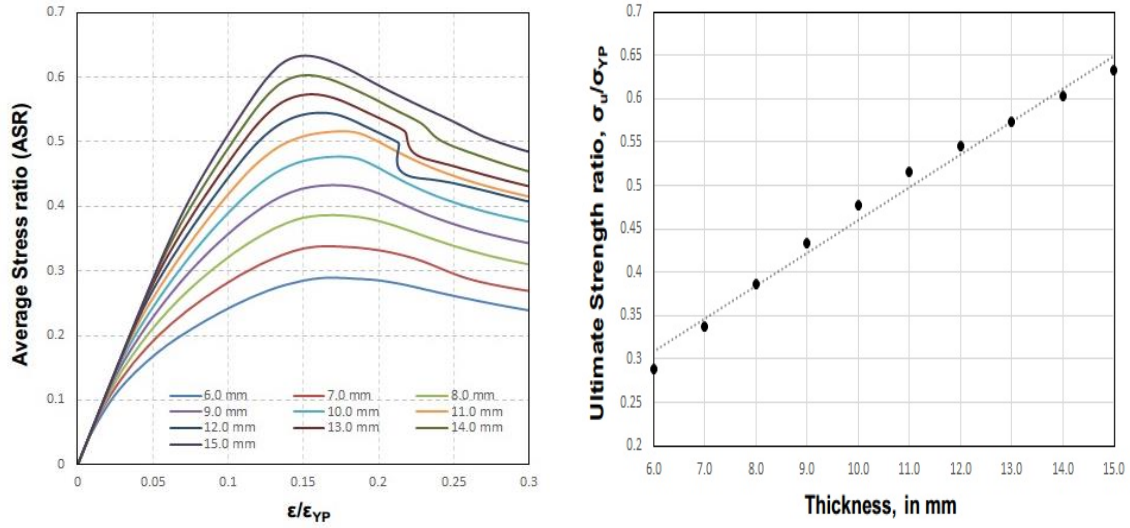

Figure 19 Stress-strain curves for different thickness (left), thickness vs ULS (right) for intact plate

The same process was conducted as well for the intact plate with the opening (Figure 20) arriving at the same solution: an increase of capacity to withstand loads and the linearly increase of collapse strength in function of bigger thicknesses.

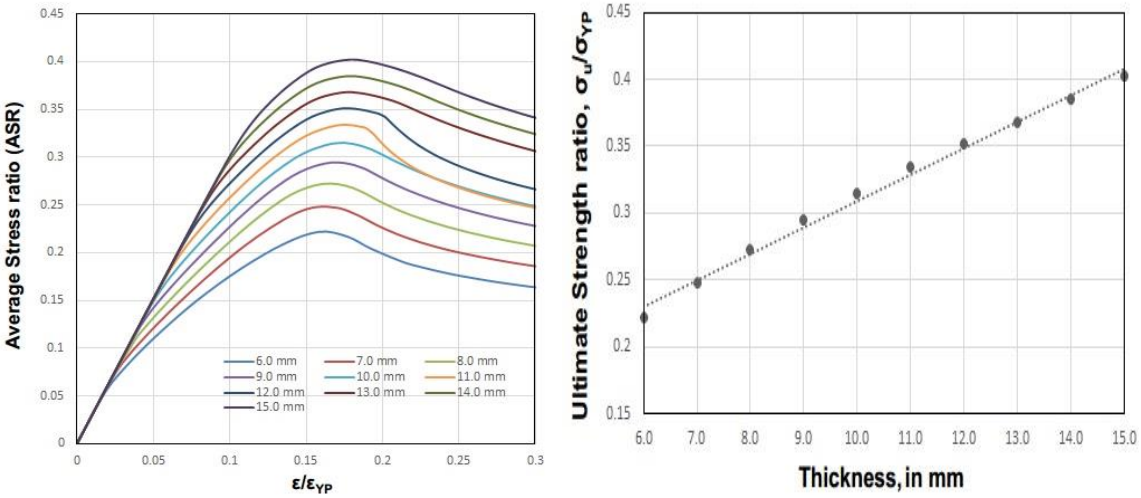

Figure 20 Stress-strain curves for different thickness (left), thickness vs ULS (right) for intact plate with opening

4.1.2 Influence of variation of opening size

Another aspect that was worth to study, it was the influence of the different sizes of the opening. For this study, it was kept constant the thickness of the plate, 10.0 millimetres, and was varied the shape of the opening. As demonstrated mathematically by Saad-Eldeen et al. (2013) and experimentally by Kim et al., (2009), the size and orientation of the opening modify significantly the ultimate capacity of the panels to withstand loads. In this case, the brief study conducted at this stage was used just to widen the possibilities and to show the effect of different sizes of opening on the selected plate (see Figure 21).

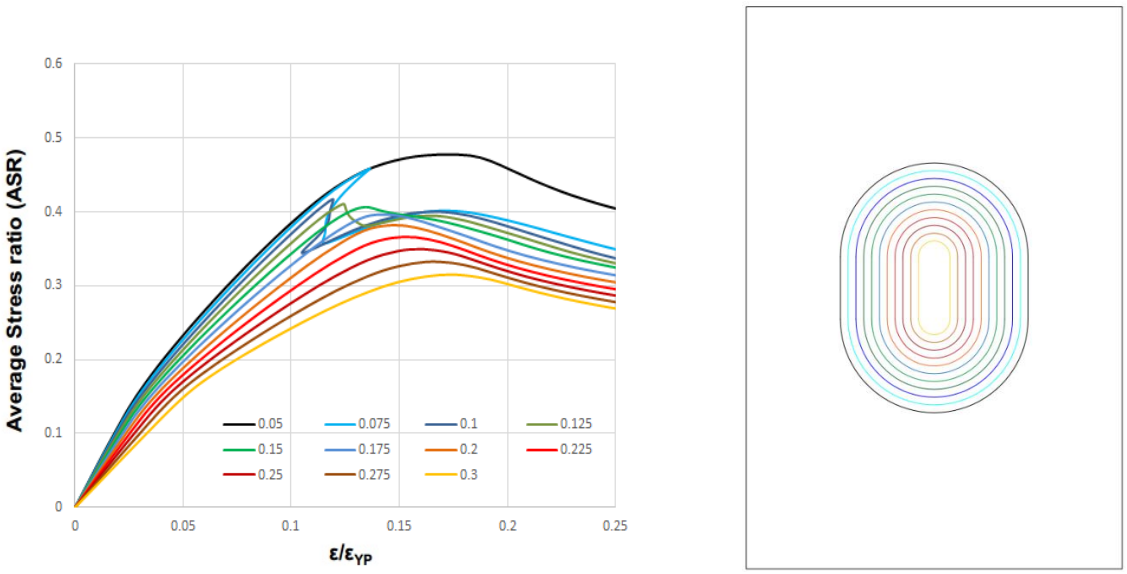

Figure 21 Stress-strain curves for different opening size (left), geometry of openings (right)

Figures 22 and 23 show how the collapse strength can be related respectively to the opening radius, as specified in the figure below, the area of the opening and the volume of the plate with an opening. It is noticeable that the collapse strength capacity linearly decreases with a major extension of opening and it increase linearly when the volume of the plate is bigger.

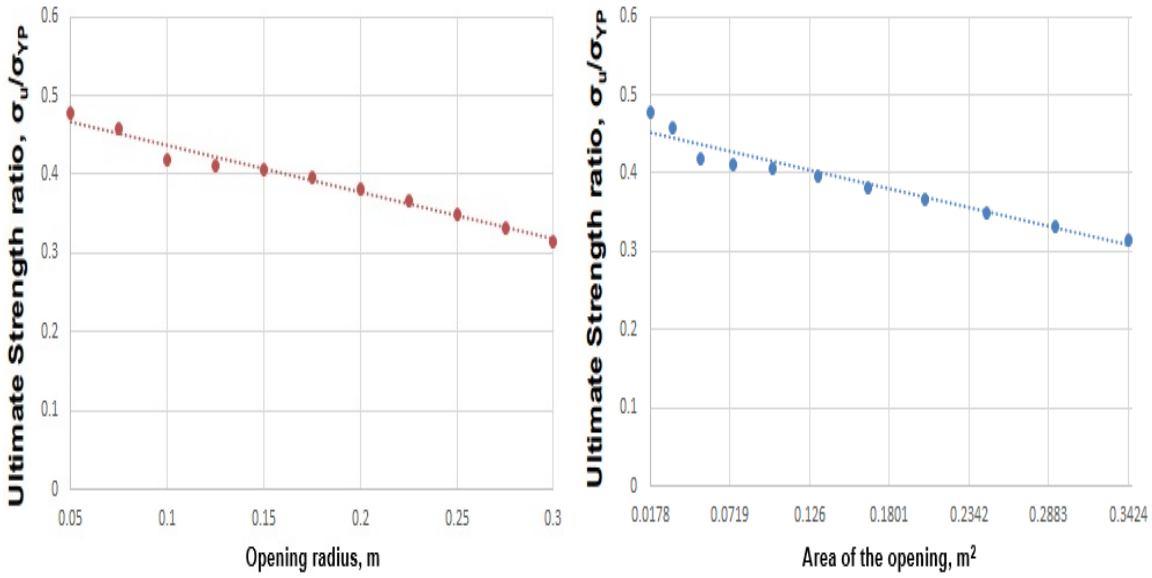

Figure 22 Opening radius vs ULS (left), Area of the opening vs ULS (right)

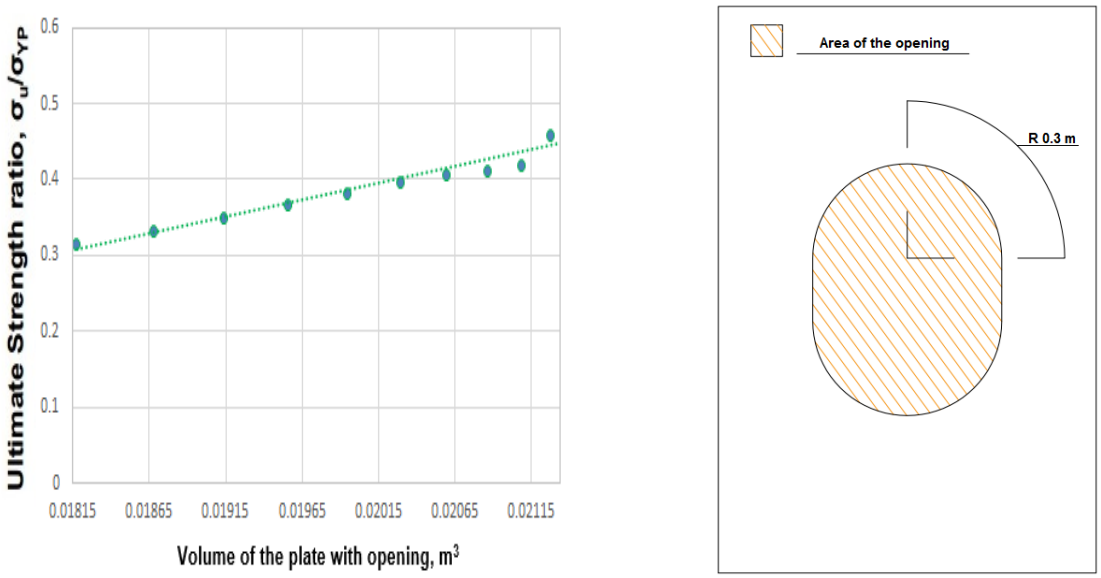

Figure 23 Volume of the plate with opening vs ULS (left), area of the opening considered (right)

The relation between the collapse strength of thinner plates can be expressed as:

$$\frac{\sigma_u}{\sigma_{YP}}(h) = -1.05\left(\frac{t_0 - t_p}{t_0}\right) + \frac{\sigma_{u,0}}{\sigma_{YP}} \tag{51}$$

With the assumption that the volume of the plate V_h with thickness $t < t_0$ is determined as follow:

$$V_h = Lbt_p - V_{hole} \tag{52}$$

4.2 Scenarios and criteria

The opening size selected for the analysis carried out in this study is a standard manhole size opening as specified by IACS Regulation with the following main parameters: the beam opening, $b_{opening}$ of 600 millimeters, length of opening, $l_{opening}$ of 800 millimeters, radius of opening, $r_{opening}$ of 300 millimeters. The assumption taken in the study, comprehend a limit for wastage allowance due corrosion for the plate, a limit for the collapse strength and selection of the position and type of reinforcement used.

4.2.1 Wastage allowance due corrosion

IACS Common Structural Rules for Bulk Carriers and Oil Tankers specifies the regulation to follow for renewal criteria (Part 1, Chapter 13). For strength assessment by Finite Element Analysis, the corrosion addition $t_{c,FEM}$ is taken equal to the canonic corrosion addition t_c determined by the following equation:

$$t_{c,FEM} = t_c = Roundup(t_{c1} + t_{c2}) + t_{res} \tag{53}$$

where $t_{c1} = t_{c2} = 0.7\ mm$ for this case study (void spaces, spaces not normally accessed), the residual thickness, t_{res} equals to *0.5* mm. IACS Rules specify as well that steel renewal is required if the measured thickness, t_m in mm, is less than the renewal thickness, t_{ren} defined as:

$$t_{ren} = t_{as-built} - t_c - t_{vol-add} \tag{54}$$

where the thickness as built of the plate, $t_{as-built}$, equals 10 mm, the voluntary addiction thickness, $t_{vol-add}$, equal to 0.5 mm. Figure 24 describes the difference between the thicknesses taken into account at design stages and in service showing the permitted wastage allowance due corrosion and the limit marked by IACS Regulation (see Figure 24).

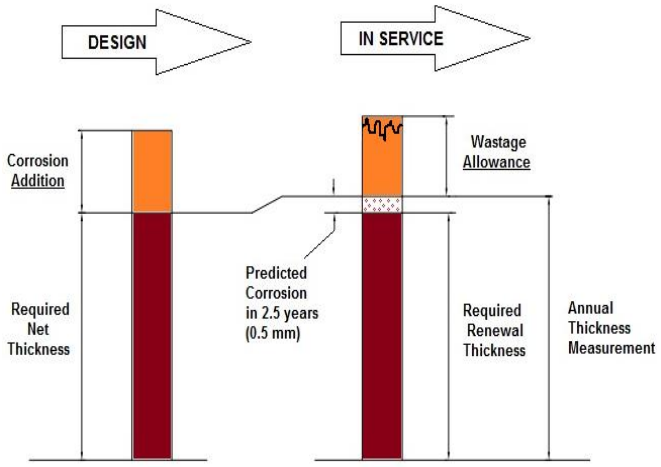

Figure 24 Design and in-service description of net thickness and wastage allowance

For this study, it was decided to discard the retrofitting process and actually replace the plate when the corrosion simulation gave a mean value for the thickness below 7.5 mm. This is due the fact that the Classification Society's Rules does not permit a lower value as exposed before.

4.2.2 Collapse strength limit

In addition to the wastage allowance due corrosion, it was decided to set a limit for the collapse strength equal to 75% of the intact plate with opening collapse strength. This limit marked the possibility and necessity to reinforce the plate to regain collapse strength with the addition of reinforcements. Figure 25 shows the stress-strain curve of the intact plate with the opening (10 mm), the maximum corroded plate with an opening (7.5 mm) and the limit of 75% for collapse strength.

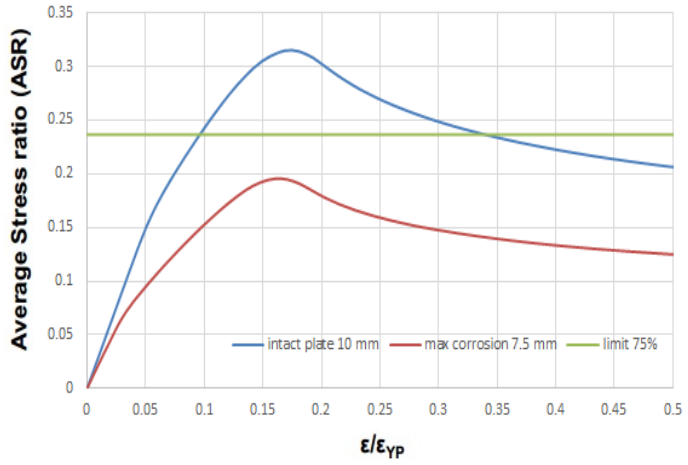

Figure 25 Stress-strain curve of intact (10 mm) and maximum corroded (7.5 mm) plate with opening

It is noticeable to observe that the stress-strain curve with the maximum wastage allowance permitted is under the limit of 75% of the collapse strength for an intact plate with an opening.

4.3 Stiffeners selection

The retrofit process has been studied preliminary with a uniform thickness equal to 8.5 millimetres due the fact that the stress-strain curve corresponding to this case is right on the limit of 75% of the collapse strength of intact plate with opening as shown in Figure 26.

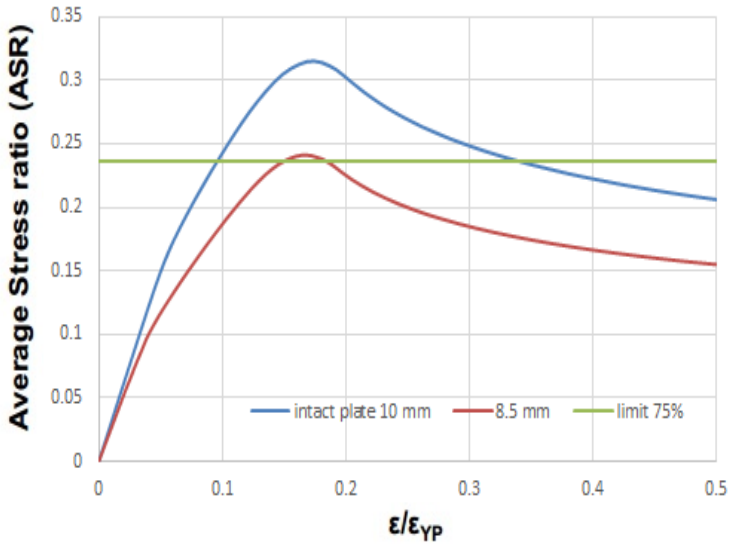

Figure 26 Stress-strain curve of intact (10 mm) and 8.5 mm plate with opening

The solutions adopted in the retrofitting process were:

- Two longitudinal stiffeners
- Two longitudinal and two transversal stiffeners
- Flange on the opening

Due to the amount of possibilities among the different stiffeners, it was decided to conduct a preliminary test to define which solutions could have been worth to study and if the one selected provides a reasonable result in regain collapse strength. The study was conducted under the assumptions that there were no residual stresses due corrosion (the welding was considered perfect and the cleaning process as well), the global and local imperfections were applied as explained in the previous chapter. It was decided to test the stiffeners at different locations to verify the contribution of each type in the recovery of the collapse strength and only the one with the highest capacity was taken into account in the final selection. The locations selected for the case "two longitudinal stiffeners" and "two longitudinal and two transversal stiffeners" has taken into account the indication from IACS Common Structural Rules about the distance between welding. In addition to that, it was decided to not place the stiffeners too close to the edges of the plate or to the opening due to excessive edge corrosion that could have caused a problem in the modelling phase. For the case "opening flange" the free edge corrosion was not taken into account and the initial imperfection considered was only the global imperfection. The stiffeners selected for the current study are indicated in the catalogue "Steel Sections for Shipbuilding" by JFE Steel Corporation.

4.3.1 CASE 1: Two longitudinal stiffeners

In the case scenario one, plate with opening reinforced with two longitudinal stiffeners, it was decided to test the following types of stiffeners (see table 5).

Table 5 Two longitudinal stiffeners scenarios tested

Scenario	Type		Location			
1	FB	50x10	[0.15-1.05]	[0.2-1.0]	[0.25-0.95]	Flat Bar
2	FB	50x15	[0.15-1.05]	[0.2-1.0]	[0.25-0.95]	Flat Bar
3	FB	100x10	[0.15-1.05]	[0.2-1.0]	[0.25-0.95]	Flat Bar
4	FB	100x15	[0.15-1.05]	[0.2-1.0]	[0.25-0.95]	Flat Bar
5	FB	150x9	[0.15-1.05]	[0.2-1.0]	[0.25-0.95]	Flat Bar
6	FB	150x15	[0.15-1.05]	[0.2-1.0]	[0.25-0.95]	Flat Bar
7	ABS	125x75x10x10	[0.15-1.05]	[0.2-1.0]	[0.25-0.95]	Unequal leg angles
8	ABS	150x90x12x12	[0.15-1.05]	[0.2-1.0]	[0.25-0.95]	Unequal leg angles
9	ABS	200x90x10x14	[0.15-1.05]	[0.2-1.0]	[0.25-0.95]	Unequal leg angles
10	ABS	250x90x10x15	[0.15-1.05]	[0.2-1.0]	[0.25-0.95]	Unequal leg angles
11	ABS	300x80x10x10	[0.15-1.05]	[0.2-1.0]	[0.25-0.95]	Unequal leg angles
12	ABS	300x100x17x11	[0.15-1.05]	[0.2-1.0]	[0.25-0.95]	Unequal leg angles
13	AB	100x100x10x10	[0.15-1.05]	[0.2-1.0]	[0.25-0.95]	Equal leg angles
14	AB	150x150x12x12	X	[0.2-1.0]	[0.25-0.95]	Equal leg angles

Figure 27 shows the model of this case and the initial imperfections considered in this case scenario.

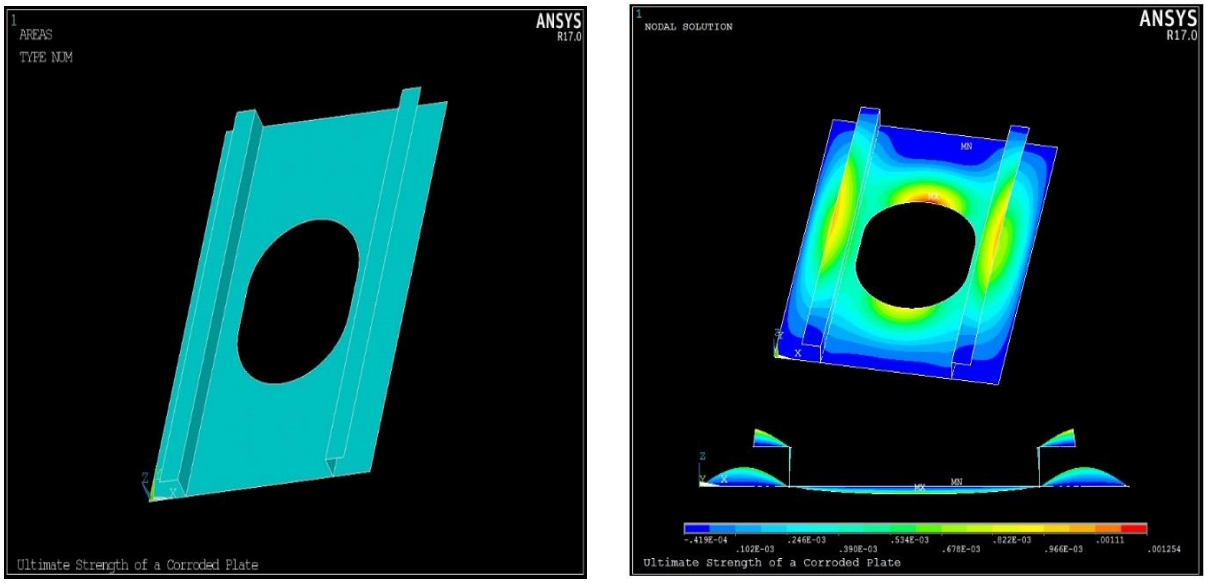

Figure 27 FEM model (left), FEM analysis and initial imperfection (right) of plate with two longitudinal stiffeners

A total of 41 simulations was carried out for this case scenario. The following table shows the maximum value of collapse strength and the location of the two longitudinal stiffeners associated with that.

Table 6 Maximum USR of every scenario and corresponding location of the two longitudinal stiffeners

Scenario	**Location**	σ_u/σ_{YP}
1	[0.15-1.05]	0.3714
2	[0.15-1.05]	0.3791
3	[0.15-1.05]	0.4135
4	[0.15-1.05]	0.4159
5	[0.2-1.0]	0.4266
6	[0.25-0.95]	0.4870
7	[0.2-1.0]	0.4896
8	[0.2-1.0]	0.5028
9	[0.25-0.95]	0.5084
10	[0.25-0.95]	0.5153
11	[0.25-0.95]	0.5302
12	[0.25-0.95]	0.4924
13	[0.2-1.0]	0.4735
14	[0.2-1.0]	0.4882

To select the three cases for the corroded plate, it was necessary to consider the weight of the two stiffeners together in function of the ultimate strength ratio, that provided an indication on which cases were worth to study both for the capacity to regain collapse strength and limited addition of weight to the plate. This last aspect was highly

taken into account for the fact that adding too much weight to one plate alone has not many consequences but the same addition to several plates could cause serious problems. Table 7 shows the weight associated with the respective stiffeners and the corresponding ultimate strength ratio. The weight is calculated considering the density of steel, δ_{steel}, equals to 7800 kg/m^3.

Table 7 Corresponding weight of stiffeners to maximum USR

Scenario	Weight [kg]	σ_u/σ_{YP}	Ratio weight/USR
1	14.04	0.3714	37.8
2	21.06	0.3791	55.6
3	28.08	0.4135	67.9
4	42.12	0.4159	101.3
5	37.908	0.4266	88.9
6	63.18	0.4870	129.7
7	56.16	0.4896	114.7
8	70.7616	0.5028	140.7
9	91.5408	0.5084	180.1
10	108.108	0.5153	209.8
11	106.704	0.5302	201.2
12	174.096	0.4924	353.6
13	56.16	0.4735	118.6
14	101.088	0.4882	207.1

Figure 28 shows the weight in function of ultimate collapse strength. It is noticeable that all the cases selected are above the limit of 75% of the collapse strength of the intact plate.

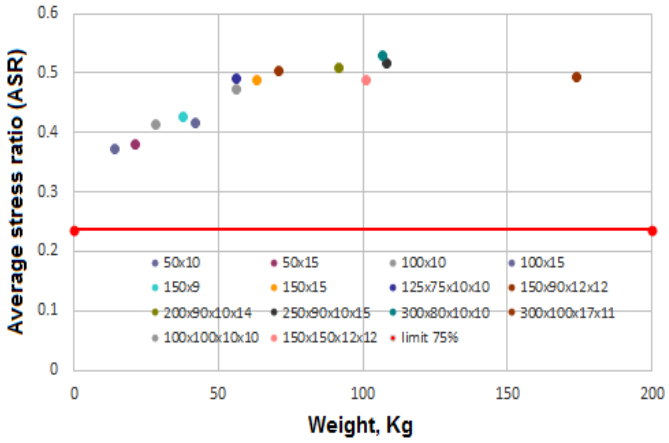

Figure 28 Diagram weight vs USR of plate with opening and two longitudinal stiffeners

The three cases selected for the retrofitting study are:

- 50x10
- 100x100x10x10

- 300x80x10x10

In particular, the stiffeners 50x10 have the lowest ratio between weight and ASR, the 300x80x10x10 have the highest capacity to regain collapse strength while the 100x100x10x10 provide a right compromise between weight and ultimate strength capacity.

4.3.2 CASE 2: Two longitudinal and two transversal stiffeners

In the case scenario two, plate with opening reinforced by two longitudinal and two transversal stiffeners, it was decided to consider only three types of stiffeners and to vary the location of the transversal ones. In addition to that, it was necessary to test different thicknesses for transversal stiffeners in the case 300x80x10x10 to check how the ultimate collapse strength could vary in function of the increased weight and thickness. Table 8 shows the different tests carried out.

Table 8 Scenarios selected for the case 2 longitudinal and 2 transversal stiffeners

	Longitudinal stiffeners	Transversal Stiffeners	Location [0.2-1.1]	Location [0.3-1.2]	Location [0.4-1.3]	
FB	50x10	50x10	X	X	X	Flat bar
AB	100x100x10x10	100x10	X	X	X	Equal leg angles
ABS	300x80x10x10	300x8			X	Unequal leg angles
		300x10	X	X	X	Unequal leg angles
		300x12			X	Unequal leg angles
		300x15			X	Unequal leg angles
		300x20			X	Unequal leg angles

Figure 29 shows the model of this case and the initial imperfections considered in this case scenario.

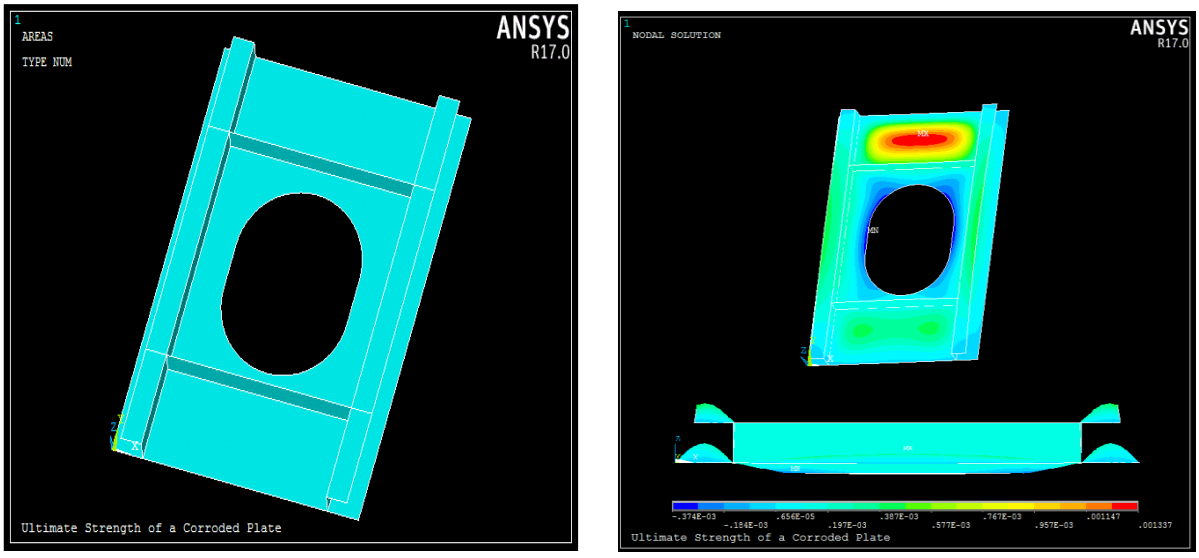

Figure 29 FEM model (left), FEA and initial imperfection (right) of plate with two longitudinal and two transverse stiffeners

A total of 13 simulations was carried out for this case scenario. Table 9 shows the maximum value of collapse strength and the location of the two transversals and two longitudinal stiffeners associated with that.

Table 9 Maximum USR and corresponding location of the transverse stiffeners

Type	Location	σ_u/σ_{YP}
2 x 50x10 + 2 x 50 x10	[0.2-1.1]	0.2507
2 x 50x10 + 2 x 50 x10	[0.3-1.2]	0.2678
2 x 50x10 + 2 x 50 x10	[0.4-1.3]	0.2947
2 x 100x100x10x10 + 2x100x10	[0.2-1.1]	0.2279
2 x 100x100x10x10 + 2x100x10	[0.3-1.2]	0.2537
2 x 100x100x10x10 + 2x100x10	[0.4-1.3]	0.2815
2 x 300x80x10x10 + 2 x 300x10	[0.2-1.1]	0.2618
2 x 300x80x10x10 + 2 x 300x10	[0.3-1.2]	0.2752
2 x 300x80x10x10 + 2 x 300x10	[0.4-1.3]	0.2988
2 x 300x80x10x10 + 2 x 300x8	[0.4-1.3]	0.2981
2 x 300x80x10x10 + 2 x 300x12	[0.4-1.3]	0.3002
2 x 300x80x10x10 + 2 x 300x15	[0.4-1.3]	0.3021
2 x 300x80x10x10 + 2 x 300x20	[0.4-1.3]	0.3027

Figure 30 shows that one case cannot be considered for the study due to the fact that the ultimate collapse strength is below the limit of 75% denoting that it is not an effective solution for the retrofitting study.

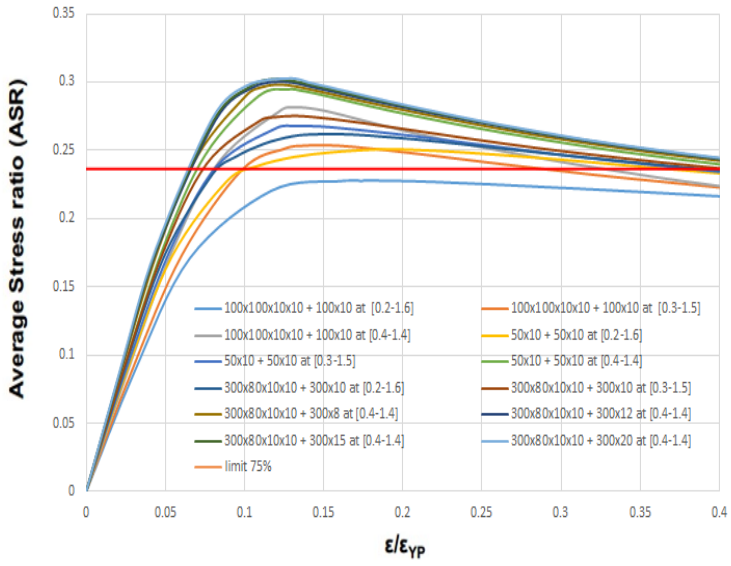

Figure 30 Stress-strain curves of plate with opening and two longitudinal and two transverse stiffeners

In this case the selected cases were four. Also for this case it was necessary to compare the weight of the stiffeners in function of the collapse strength. Table 10 and Figure 31 show the weight/ASR ratio and give an indication on which solutions were worthy to study.

Table 10 Corresponding weight of stiffeners to maximum USR

Type	Weight [kg]	σ_u/σ_{YP}	Ratio weight/USR
50x10 + 50x10 at [0.2-1.6]	21.06	0.2507	84.0
50x10 + 50x10 at [0.3-1.5]	21.06	0.2678	78.7
50x10 + 50x10 at [0.4-1.4]	21.06	0.2947	71.5
100x100x10x10 + 100x10 at [0.2-1.6]	68.64	0.2279	301.2
100x100x10x10 + 100x10 at [0.3-1.5]	68.64	0.2537	270.5
100x100x10x10 + 100x10 at [0.4-1.4]	68.64	0.2815	243.9
300x80x10x10 + 300x10 at [0.2-1.6]	139.46	0.2618	532.6
300x80x10x10 + 300x10 at [0.3-1.5]	139.46	0.2752	506.8
300x80x10x10 + 300x10 at [0.4-1.4]	139.46	0.2988	466.8
300x80x10x10 + 300x8 at [0.4-1.4]	132.91	0.2981	445.8
300x80x10x10 + 300x12 at [0.4-1.4]	146.02	0.3002	486.4
300x80x10x10 + 300x15 at [0.4-1.4]	155.84	0.3021	515.9
300x80x10x10 + 300x20 at [0.4-1.4]	172.22	0.3027	568.9

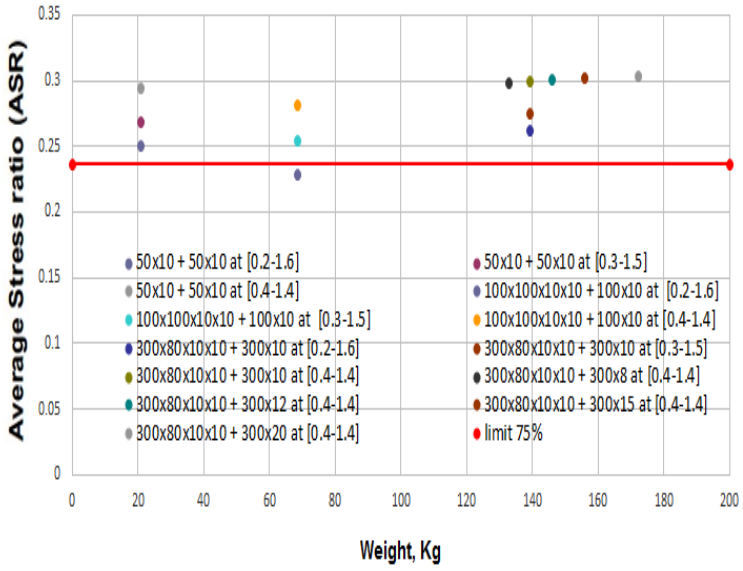

Figure 31 Ultimate strength ratio vs weight of plate with opening and two longitudinal and two transverse stiffeners

It is noticeable to observe that the positioning of the transverse stiffeners influences the collapse capacity of the system plate-stiffeners, in particular more the transverse stiffeners are placed far away the edges of the plate, more the average stress ratios increase. It is also important to remark that the three different types of stiffeners cannot be compared among themselves due to the spacing between longitudinal stiffeners is different. In fact, a wider spacing comports a longer transverse stiffener and a consequent increase of weight (see Figure 32).

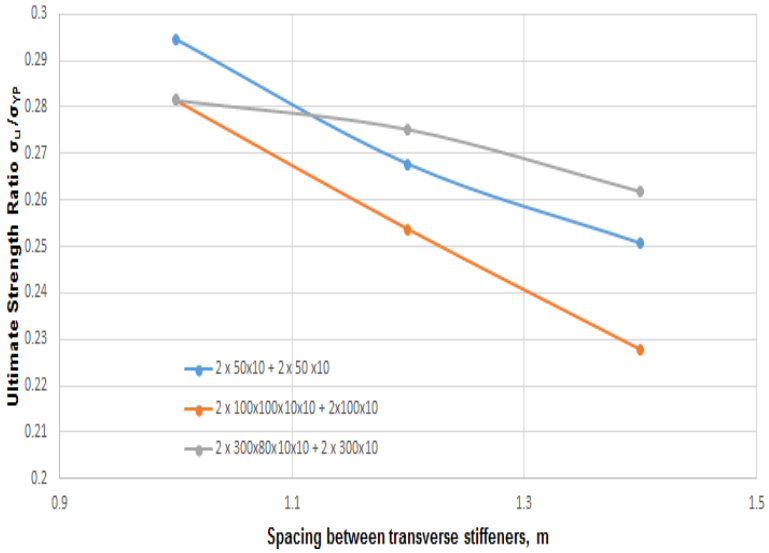

Figure 32 Ratio between transverse spacing and USR

As well, for the case 2 x 300x80x10x10 + 2 x 300x*n*, with *n* varying between 8 and 20 millimetres, it can be observed that the collapse capacity slightly increases as shown in Figure 33.

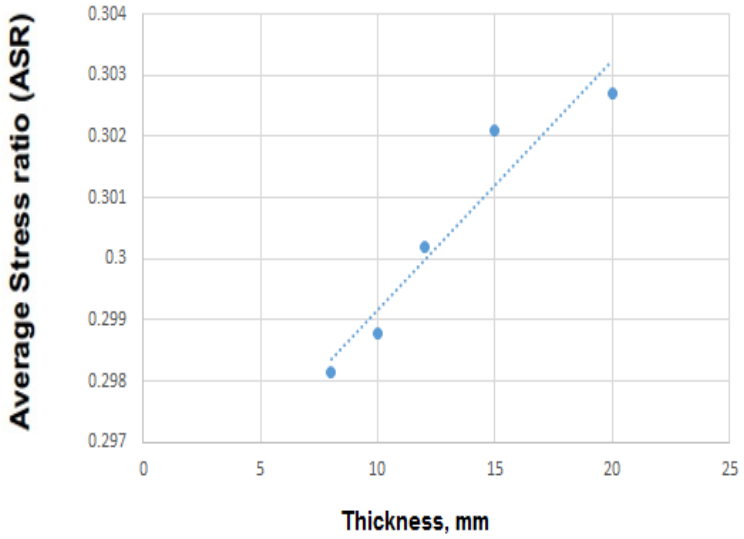

Figure 33 Thickness vs USR

The four cases selected for the retrofitting study are:

- 2 x 50x10 + 2 x 50x10 at [0.4-1.4]
- 2 x 100x100x10x10 + 2 x 100x10 at [0.4-1.4]
- 2 x 300x80x10x10 + 2 x 300x8 at [0.4-1.4]
- 2 x 300x80x10x10 + 2 x 300x20 at [0.4-1.4]

In this case scenario, it was decided to take into account the solutions that provide the highest collapse strength capacity for each group of stiffeners.

4.3.3 CASE 3: Opening flange

In the case scenario three, plate with opening reinforced with flange, it was decided to test thirteen different flat bars as shown in Table 11.

Table 11 Selected scenarios for flange on the opening

FB 100x10	Flat bar
FB 100x20	Flat bar
FB 125x10	Flat bar
FB 125x20	Flat bar
FB 150x9	Flat bar
FB 150x12	Flat bar
FB 150x20	Flat bar
FB 200x10	Flat bar
FB 200x20	Flat bar
FB 250x10	Flat bar
FB 250x25	Flat bar
FB 300x10	Flat bar
FB 300x17	Flat bar

For stiffeners with dimensions below 100x10 it was impossible to carry out an effective analysis due to geometry failure of the model given by excessive distortions.

Figure 34 shows the model used for the analysis and the initial imperfection applied to the plate. In particular, it was considered that the flange has been welded to the edge of the opening and the welding itself does not contribute to a local imperfection of the plate in any direction.

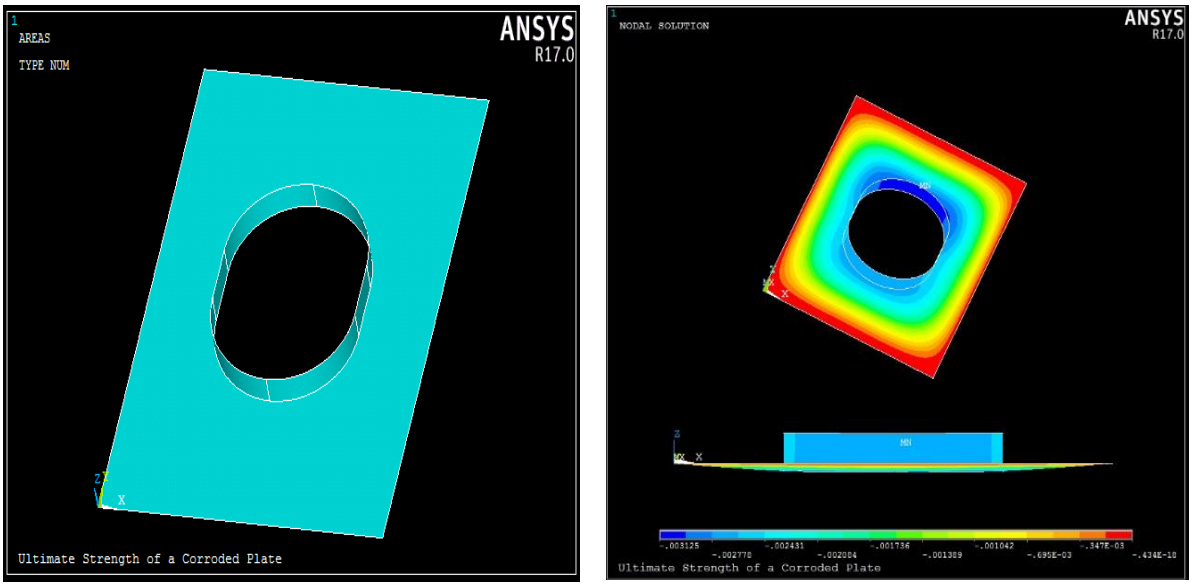

Figure 34 FEM model (left), FEM analysis and initial imperfection (right) of plate with flange on the opening

A total of 13 simulations was carried out in this case scenario. Table 12 and Figure 35 show the maximum value of collapse strength and the weight associated with the respective flange.

Table 12 Corresponding weight of flange to maximum USR

	Weight [kg]	σ_u/σ_{YP}	Ratio weight/ASR
100x10	17.82	0.330503	53.9
100x20	35.63	0.335362	106.2
125x10	22.27	0.331105	67.3
125x20	44.54	0.336663	132.3
150x9	24.05	0.331011	72.7
150x12	32.07	0.333308	96.2
150x20	53.45	0.337617	158.3
200x10	35.63	0.333331	106.9
200x20	71.26	0.339050	210.2
250x10	44.54	0.334852	133.0
250x25	89.08	0.341096	261.1
300x10	53.45	0.336258	158.9
300x17	90.86	0.340499	266.8

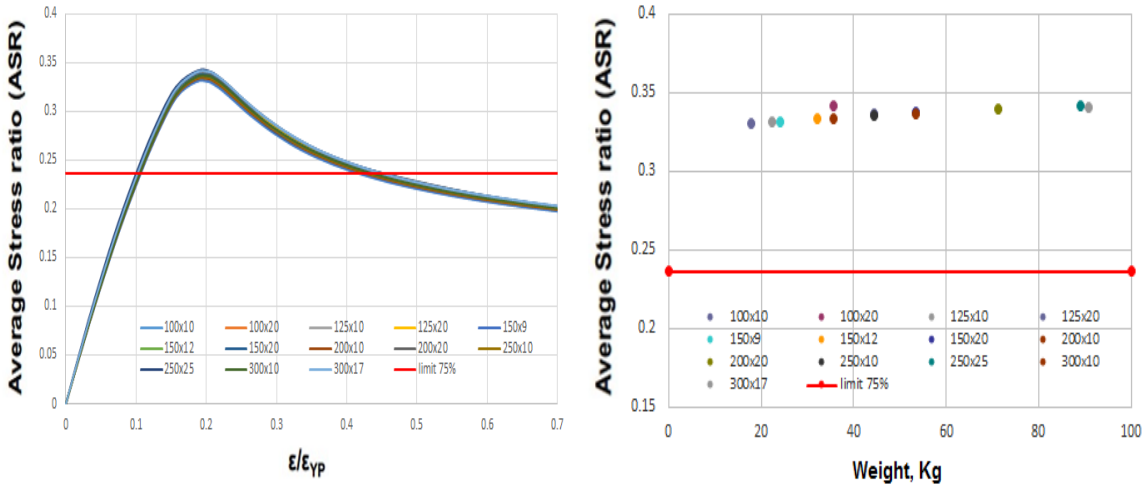

Figure 35 Stress-strain curve of plate with opening with flange on the opening (left), Weight vs USR (right)

It is noticeable to observe that collapse strength increases more with bigger thicknesses of the same type of stiffeners than an increase of the size of the thickness itself as shown in Figure 36.

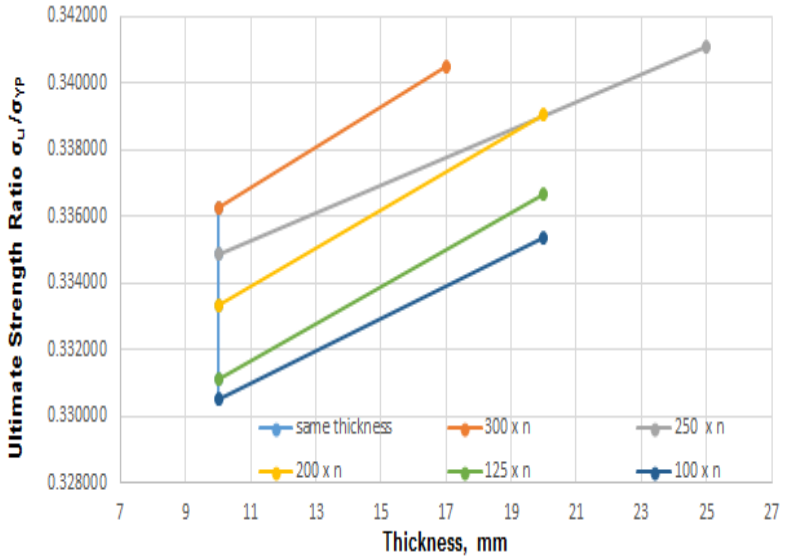

Figure 36 Thickness vs USR

Different stiffeners with the same thickness increase linearly the collapse capacity, but the growth is more sensible with a change of the thickness of the same flat bar type. In this case *n* is assumed as the different thickness specified in the stiffener type table. The three cases taken into account for the retrofitting study are:

- 100x10
- 200x10
- 300x17

Respectively having: the first lowest ratio between weight and ASR, the second an average mean value and the third having the highest ratio.

5 Retrofitting Assessment

Classification Societies mark the wastage allowance for a corroded steel plate and indicates the guidelines to follow for repairs. In the majority of the cases, it is recommended to substitute the steel panel with a new one when the thickness of the plate, measured at three different points on it, is under the required net thickness. Actually also when a plate is severely corroded, the usual procedure is to add new material to the plate or to substitute it to regain collapse strength capacity. The numerical experiment carried out in this study has the prerogative to find a different solution to this problem demonstrating that a corroded plate, treated with new coating and the addition of reinforcement, can actually withstand the load and permits a longer service life of the original plate. As stated in DNV *Sec.4 Allowable material diminution for general corrosion* "Areas found with diminution in excess of acceptable limits are normally to be repaired with inserted material of same grade and scantlings as original. Alternative dimensions, materials and repair methods may, however, be accepted provided they are specially considered and approved, typically in connection with refined minimum thickness calculations" giving possibilities to find different solutions to the corroded plate.

The numerical experiment consists in a series of finite element simulations of a corroded plate with opening to which are applied different reinforcement profiles as stated in the previous chapter. The following assumptions were adopted in the study:

- Random, non-uniform and time dependent corrosion with the presence of 0% of pits
- Perfect welding between stiffeners and plate
- Perfect cleaning after repair

It was decided at first to carry out the study with the randomized, non-uniform and time dependent corrosion due the fact of lack of experimental data to be used in the study due the size of the panel and opening. The model used, Garbatov et al. (2007), gives a reasonable simulation of a time dependent corrosion of the plate.

Perfect welding was adopted to limit the initial imperfection of the plate only to global and local imperfections, as stated in the previous chapter, assuming that there are not residual stressed caused by the welding process and also that the welding work create a flawless joint between plate and stiffeners. This last aspect is really important because a non-perfect interaction between plate and stiffeners may cause an early failure of the system plate-stiffeners and a reduction collapse capacity.

Perfect cleaning was assumed from the fact that it will permit a stop in the corrosion process. The new coating life (4 years) was taken less than 1/3 of the initial coating life (10.54 years) giving a reasonable assumption for the time dependent quality of the coating after the repair.

The limits adopted for the numerical experiment for each scenario were:

- 75% of the ultimate strength capacity of the intact plate
- Required net thickness

In particular, once the average thickness of the plate analysed is under the required net thickness, the plate had been substituted as stated by Classification Society Rules. The limit of 75% of ultimate strength capacity of intact plate marked the limit at which the plate had to be reinforced to regain collapse strength capacity. Figure 37shows the time dependent corrosion history of the plate with the opening.

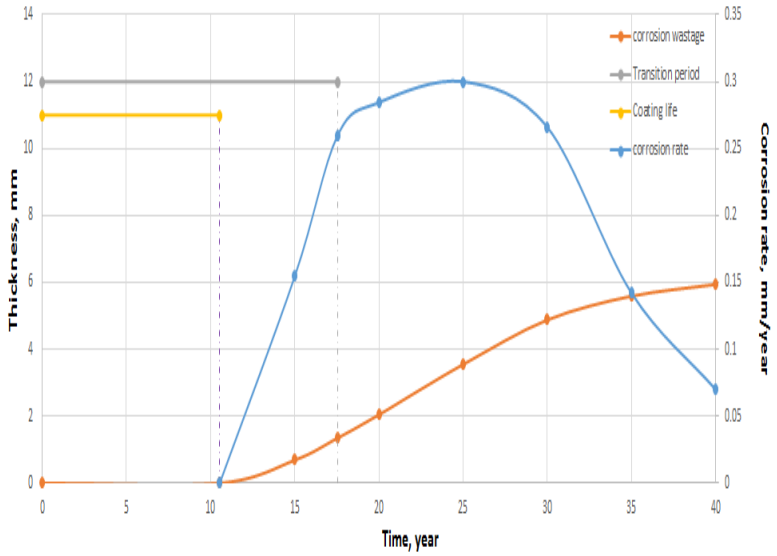

Figure 37 Time history of corrosion wastage and corrosion rate

It can be observed that there is a rapid growth in the corrosion rate after the end of the effectiveness of the coating applied to the plate. This growth continues after the transition time and then decreases. This behaviour can be explained with the fact that, after the 25th year, the plate is severely corroded and the residual thickness is way lesser than the original, leaving less material to be corroded.

Also, the corrosion effectiveness is not that rapid as before, taking more time to corrode material.

On the other hand, the corrosion wastage follows the theorized pattern, but with a slower growth. Anyways, it kept the asymptotic behavior corresponding to a stabilization of the corrosion and a lower corrosion rate.

In Figure 38 it can be observed the thickness time history of the same panel without retrofitting process.

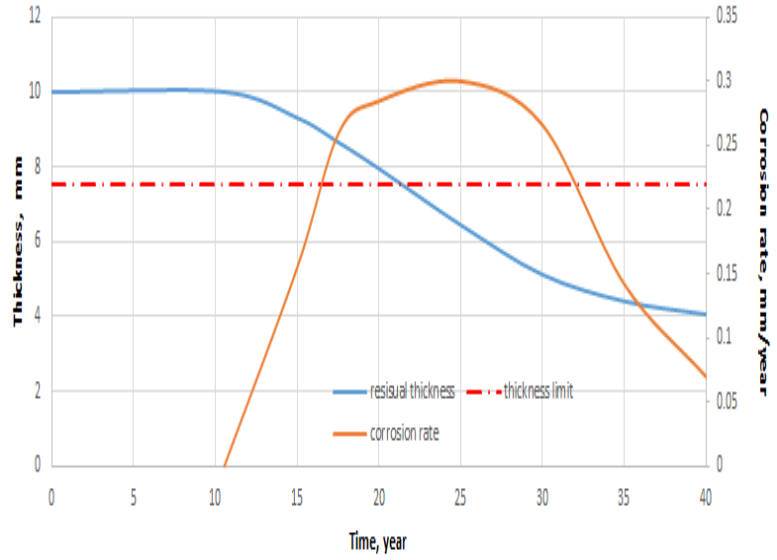

Figure 38 Time history of residual thickness and corrosion rate

It can be observed that theoretically the plate is not any more effective for Classification Society after the 21th year. However, for the other limiting parameter, limit of 75% of ultimate strength of the intact panel with opening, the effectiveness is lost previously, between the 18th and 19th year, as shows in Figure 39.

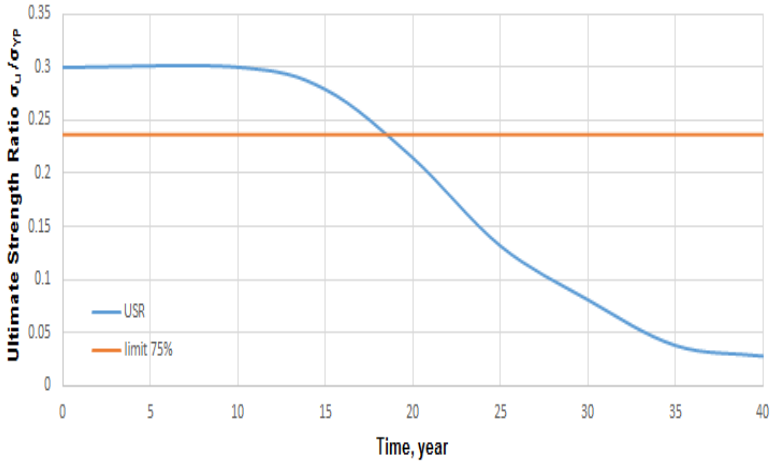

Figure 39 Time history of ultimate strength ratio of plate with opening under random, non-uniform random corrosion

The retrofitting assessment has been carried out with a series of ten finite element analysis every year for each stiffener selected. The total number of simulations is 1273, with only 400 actually have given solution. It was decided to mark the year 20th as the year at which the simulations start. The study has been carried out applying the corrosion of the plate of the 19th year with the addition of stiffeners. Furthermore, a cleaning process of the panel was made and a new coating was applied to the plate. This permits to assume that the corrosion is stopped for the time period the coating is effective. The new coating life considered in the study had a life of four years (from year 19th to 23rd) with the year 24th the starting of the new corrosion process. The average thickness of the plate with an opening retrofitted is shown in the diagram below. It can be observed that the substitution of the entire plate occurs at the 26th year when the average thickness of the panel is below the limit marked by the Classification Society (see Figure 40).

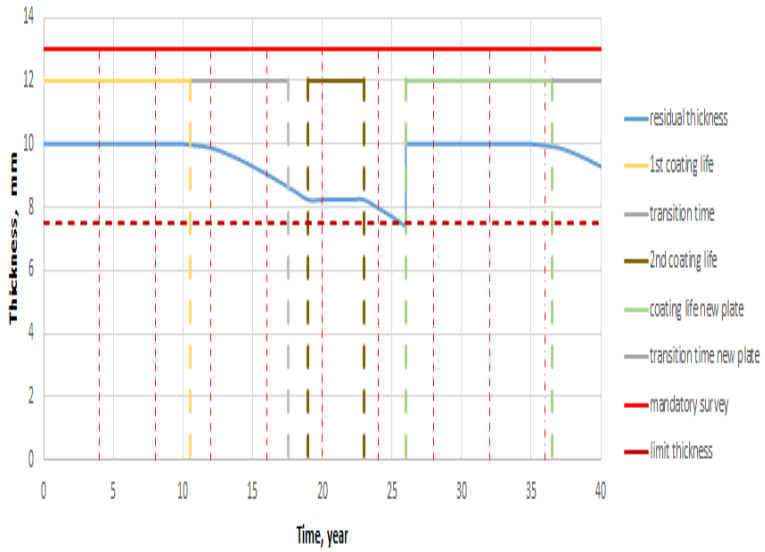

Figure 40 Time history of residual thickness of plate with opening under random, non-uniform corrosion

5.1 CASE 1: Two longitudinal stiffeners

The addition of two longitudinal stiffeners to the plate with opening increases significantly the collapse strength capacity of the panel. In particular, it is important to observe that the capacity to withstand load is greater than the one of intact plate. Figure 41 shows the results obtained from the three different solutions adopted for the case scenario one in the time period of interest (19th to 26th year).

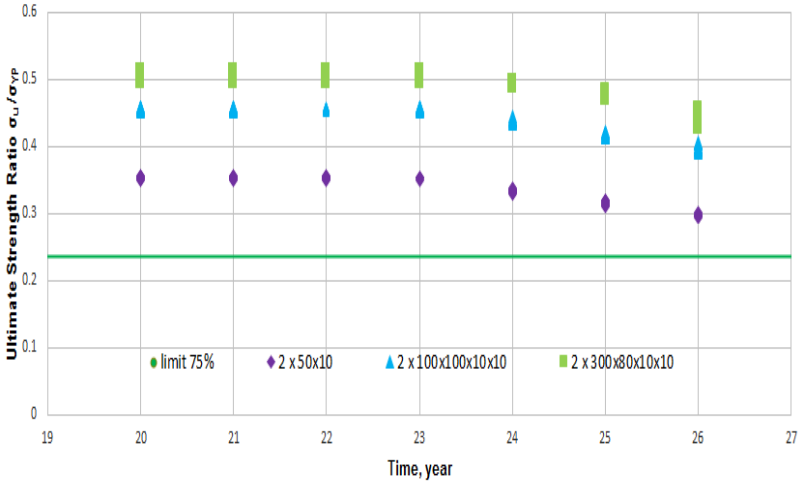

Figure 41 Variation in time of USR of corroded plate with opening retrofitted with two longitudinal stiffeners

It can be observed that with the addition of the stiffener, the plate regains collapse strength capacity. The amount of capacity recovered is greater than the value of the intact plate. The contribution of the two longitudinal stiffeners offers a reliable solution to the retrofitting problem. Figure 42 describes the behavior of the three solution in comparison to the corroded plate.

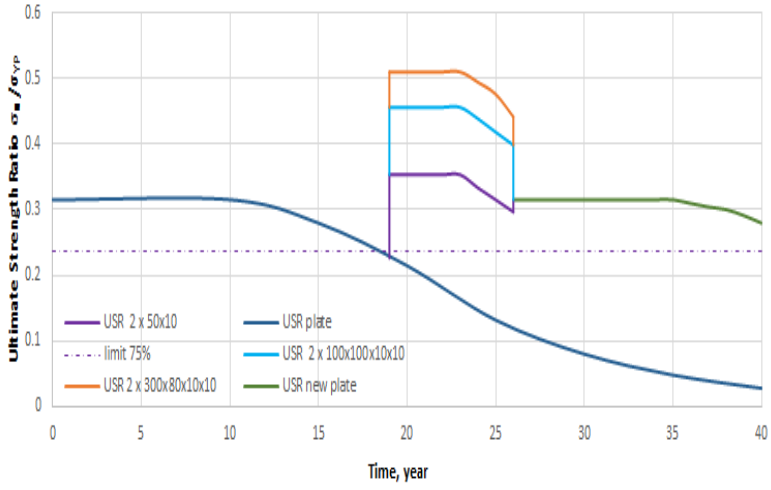

Figure 42 Retrofitting time history of 2 longitudinal stiffeners scenarios

The ultimate strength ratio curves of the three solutions adopted do not cross the limit of 75%, but it was needed to substitute the plate due to low value in residual thickness. The system corroded plate-stiffeners still had enough capacity to withstand the load applied. This gives an idea of the aspect that concern the cleaning and coating process: improving them, it is possible to prolong further the service life of the plate, reducing the cost for the replacing of the panel.

5.2 CASE 2: Two longitudinal stiffeners and two transverse stiffeners

The system of two longitudinal and two transverse stiffeners confers to the plate a limited recovery of the collapse capacity. The principal cause is given by the transverse members that significantly weaken the propriety of the panel, as explained in the previous chapter. From Figure 43, it can be observed that the retrofitted panel does not comply with the limit of 75% of an intact plate ultimate strength at year 25th, for three solutions, and year 26th, for one solution.

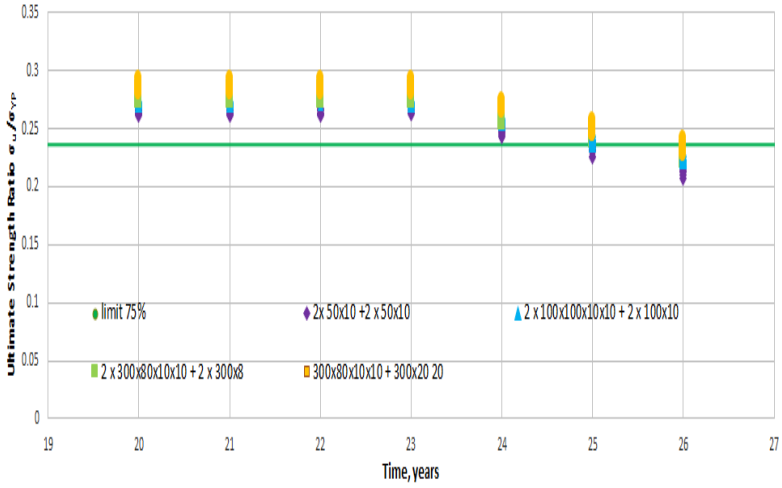

Figure 43 Variation in time of USR of corroded plate with opening retrofitted with two longitudinal and two transverse stiffeners

The limited ultimate strength capacity recovered affects also the earlier substitution of the plate for 2 scenarios, but the main problem resides in the amount of material used in the retrofitting process that a not convenient solution to the problem. Figure 44 describes the behavior of the four solutions in comparison to the corroded plate.

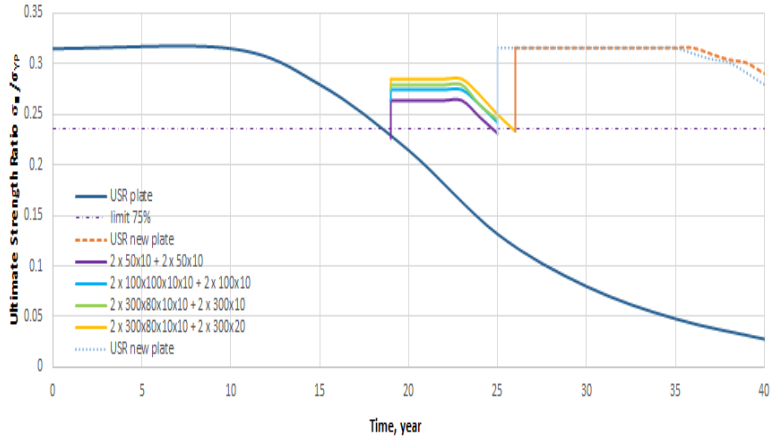

Figure 44 Retrofitting time history of 2 longitudinal and 2 transverse stiffeners scenarios

A purely valuation of the ultimate strength capacity denotes an actual acceptable solution for the four-different case scenario. On the other hand, the material used to regain the capacity of the plate is quite high as it will be described in the next chapter. The service life of the corroded panel has been improved of five years for three scenarios and for six years for one scenario. As for the case one, the substitution of the panel occurs only on one solution due to the crossing of residual thickness, in all the other cases the substitution occurs a year before the

crossing of that limit. A better cleaning and coating process can improve also in this case the service life of the panel.

5.3 CASE 3: Flange on the opening

The flange placed on the opening of the plate confers a regain of collapse strength of the same order of the intact panel. It is also important to observe that the different dimensions of the different flanges tested, increase slightly the capacity of the plate to withstand loads. This fact can be explained principally with the positioning of the reinforced member. The thickness of the flange influences more the regain of collapse strength than the height of the stiffeners itself. Figure 45 shows the results obtained from the finite element analysis.

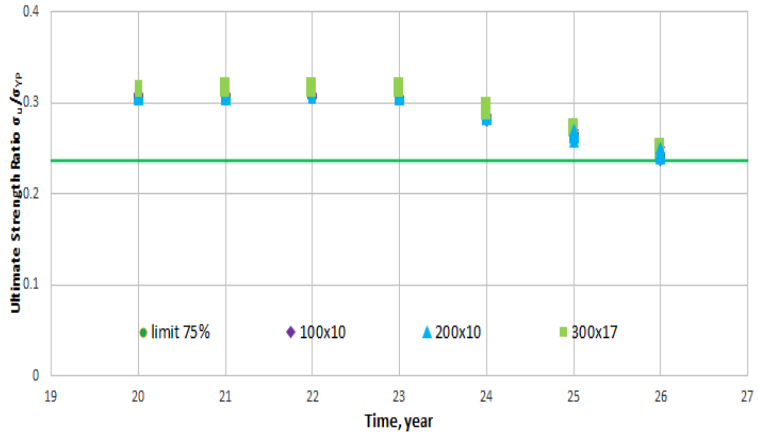

Figure 45 Variation in time of USR of corroded plate with opening retrofitted with flange on the opening

This solution provides an improvement of service life of the plate up to the 26th year. It can be observed, at that year, the ultimate strength capacity reached the limit of 75%, meaning that the substitution of the panel cannot be postponed. In addition to that, also the thickness limit is reached at the same year as shown in Figure 46.

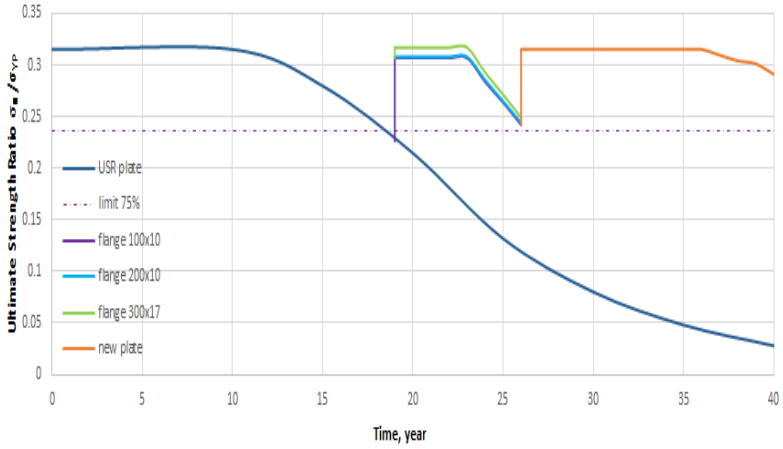

Figure 46 Retrofitting time history of flange on the opening scenarios

This solution provides a good compromise between the recovery of the collapse strength capacity that can be improved with a better cleaning and coating of the plate. The service life of the plate has been improved by 6 years, reaching the limit both for the 75% and residual thickness.

6 Weight Assessment

When a steel plate is starting to corrode, it loses material and in consequence weight. The study and control of weights in a marine structure has a great impact on the capacity to carry cargo. A great improvement of the weight of a single panel will not create relevant changes, but it is important to think that corrosion appears on different members and the sum of all of them, at the end, has serious influence. For this reason, a weight study had been carried out to determine which solution of the scenarios tested is more reasonable to adopt (see Figure 47).

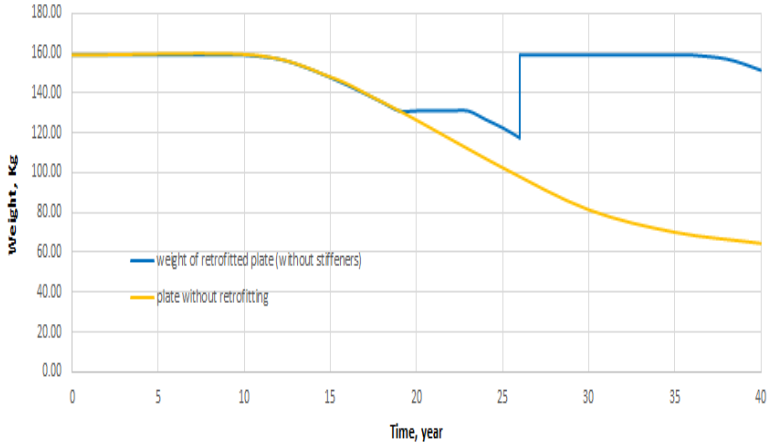

Figure 47 Weight time history of plate with opening

It can be observed that there is a discrepancy between the intact plate and the retrofitting of about 40 kilos. This value can be used as a reference to check if the stiffeners selected for the testing can actually limit the added weight of the panel. It is important to remark that in this study is not taken into account the additional weight of the new coating film applied, but just the net weight of the plate, by reinforced members and of the welding between panel and stiffeners. The type of welding taken into account for the study is manual Shielded Metal Arc Welding (SMAW).

6.1 Weight of welding

The weight of welding is directly a function of the length of the welding and thickness. It was decided to consider the welding continuous and on both sides of the stiffener. Considered the reinforced profiles already bought assembled, the welding presents in this study are the connections between panel and stiffeners.

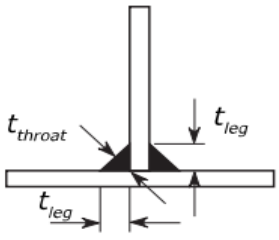

Figure 48 Definition of throat thickness and thickness leg (DVN-GL)

The indication of length and thickness of welding is in DNV-GL Classification Society Rules (Part 3, Chapter 13: Welding). The main parameter is the thickness leg, t_{leg} , (see Figure 48), defined as:

$$t_{leg} = f_c \, f_1 \, f_2 \, t_w \tag{55}$$

where f_c is a coefficient depending on environment, f_1 is a coefficient depending on the welding type, f_2 is a coefficient depending on the edge preparation and t_w is the effective thickness of the abutting plate.

The weight of welding is a function of the length and of the thickness leg. The three different cases present different thicknesses of reinforced members and as well length. For the different thickness has been decided to take a conservative approach and to round up the thickness leg. The "Handbook of Welding" gives values of the weight of weld (kg/m) in function of t_{leg}. Table 13 shows the conservative approach used.

Table 13 Angle of thickness throat and corresponding thickness of welding material (DNV Welding)

standard	
T	
mm	45°
3.18	0.04
4.76	0.089
6.35	0.158

study cases			
T			Stiffener thickness
mm	45°		
2.88	0.04	->	8 mm
3.6	0.089	->	10 mm
6.12	0.158	->	17mm

Those values are independent of the type of welding used, but only by the weld metal for fillet welds and elements of common butt joints. In further works, it will be necessary to take into account the quality and type of welding. Figure 49 presents the two-different type of welding taken into account in this study.

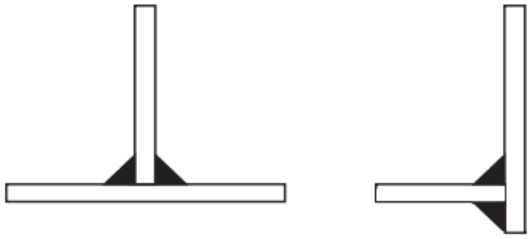

Figure 49 Type of welding considered in the study: longitudinal and transverse stiffeners (left), flange on the opening (right)

6.1.1 CASE 1: Two longitudinal stiffeners

The two longitudinal stiffeners increase the total weight of the plate starting the year 19th, when the retrofit process occur, until year 26th, substitution of the panel. Figure 50 describes the increasing of weight of the system plate-stiffeners in the time period of study.

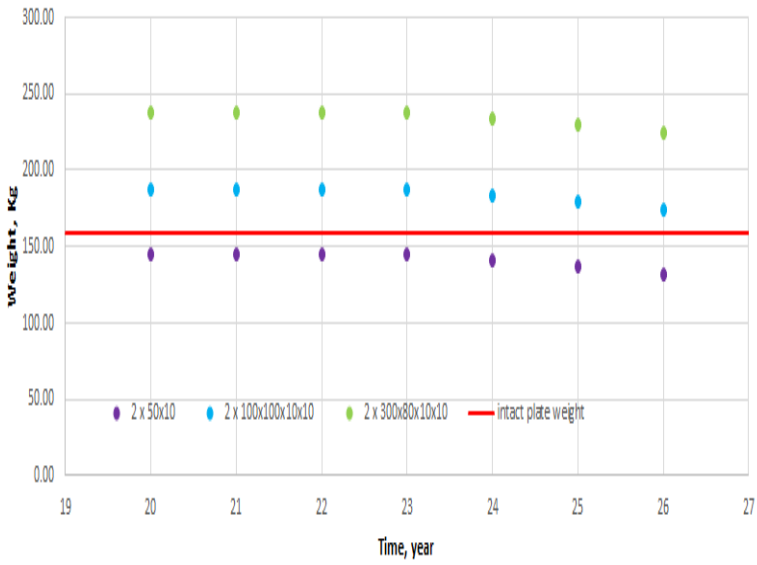

Figure 50 Variation in time of weight of corroded plate with opening retrofitted with 2 longitudinal stiffeners

Only the stiffeners with flat bar profile 50x10 remains under the intact plate weight, the other two scenarios surpass that limit adding sensible weights to the panel. The reinforced profiles 100x100x10x10 add in total 18% of mass to the plate, while the 300x80x10x10 add 49%. At parity of the collapse strength regain and depending by the actors involved, the owner of a marine structure or shipyard, it might be convenient to adopt one solution or the other. Obviously, the weight affects as well the cost of the retrofitting process as will be explained in the next chapter.

6.1.2 Two longitudinal stiffeners and two transverse stiffeners

The scenario with two longitudinal and two transverse stiffeners resulted to be the most critical one in regain of the collapse strength. More elements added to the plate means more weight as well. Figure 51 describes the increasing of weight of the system plate-stiffeners in the time period of study.

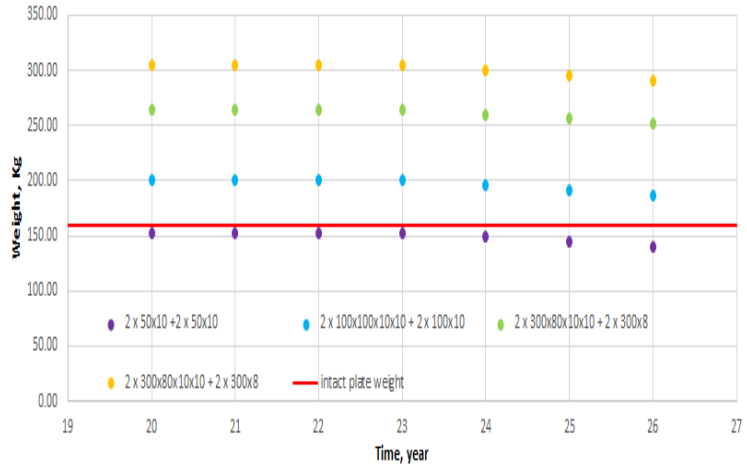

Figure 51 Variation in time of weight of corroded plate with opening retrofitted with 2 longitudinal and 2 transverse stiffeners

It can be observed that the four profiles 50x10 remain below the intact plate weight with an actual decrease of 4% of that mass. The other three scenarios increase sensibly the weight of the order, respectively, by 26%, 66% and 91% of the initial panel mass. It can be affirmed that those case scenarios are not a viable way to retrofit the panel due the excessive weight and a limited regain in collapse strength capacity.

6.1.3 CASE 3: Flange on the opening

The case flange on the opening has reasonable limited overall dimension compared to the other two, however the 300x17 flange, due to its thickness, increases sensibly the added mass to the system plate-flange. Figure 52 shows the increasing of the weight of the system plate-stiffeners in the time period of study.

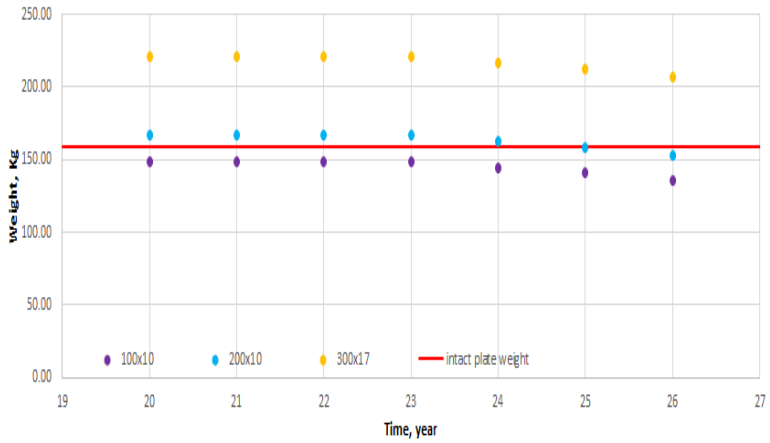

Figure 52 Variation in time of weight of corroded plate with opening retrofitted with flange on the opening

The profiles 100x10 and 200x10 are close to the intact plate weight is giving an ideal solution to the retrofitting problem. The flange 300x17 is actually over dimensioned and it is not a viable solution, also compared to the tight difference in collapse strength capacity between the scenarios. The percentage of the added weight are on the order of -6.5%, 4.5% and 38%.

7 Economical Assessment

Connected to the weight there is also the economic assessment. Every profile used as a cost associated. Furthermore, the cleaning, coating and welding processes, increase the cost that has to be destined to the retrofitting of the plate. In addition to that has to be considered the cost associated to work performed by workers, transport of material, electricity, administrative costs and others. The following formula has been used to obtain a reasonable value of cost associate to retrofitting process.

$$CAPEX = \{W_{stiff} * C_{steel} + C_{weld} * l_{weld} + C_{workers} * H_{work}\} * (1 + C_{profit} + C_{overhead}) \quad (56)$$

where W_{stiff} is the weight of the stiffener used in the retrofitting process, C_{steel} is the cost of the material of the stiffeners, in this case steel, C_{weld} is the cost of the welding material used, l_{weld} is the length of the welds, $C_{workers}$ is the cost of one hour of labor, H_{work} is the number of hour needed to complete the process, C_{profit} is the profit of the shipyard and $C_{overhead}$ is the overhead cost that covers transportation, cleaning, new coating, electricity, etc.

For this study, the price of steel has been taken equal to 700 €/ton; the total cost of welding is given by different factors, reassumed in the table below; the hour of work is direct function of the time needed to do the welding process; the cost of workers as been taken equal to 20 €/hour (this value can vary sensibly depending where the retrofitting process has been commissioned with a difference from 4 €/hour to 40 €/hour); the cost of profit has been taken as 5% and the overhead as 30%. The cost of profit and the overhead cost are also sensible to the location where the retrofitting process has been done (see Table 14).

Table 14 SMAW cost in dollars per feet (NAVYBMR)

Process Method of Welding	SMAW Manual
Electrode Diameter (in)	3/16
Welding Current (amps)	250
Welding Voltage (volts)	25
Travel Speed (in/min)	9
Welding Time (hr)	0.063
Arc Time (hr)	0.022
Labor + Overhead Cost ($/hr)	18
Operator Factor (%)	35
Weight of Deposit (lbs)	0.106
Electrode Cost ($/lbs)	0.45
Deposition Efficiency (%)	72
Deposition Rate (lbs/hr)	4.8
Electric Power Cost ($/kw/hr)	0.035
Power Source Efficiency (%)	50
Overhead Cost ($/ft)	1.136
Electrode Cost ($/ft)	0.066
Shielding Gas Cost ($/ft)	
Electric Power Cost ($/ft)	0.01
Total Cost ($/ft)	**1.212**

7.1 CASE 1: Two longitudinal stiffeners

The total cost associated with the retrofitting process of deteriorated plate with opening with two longitudinal stiffeners is shown in Figure 53.

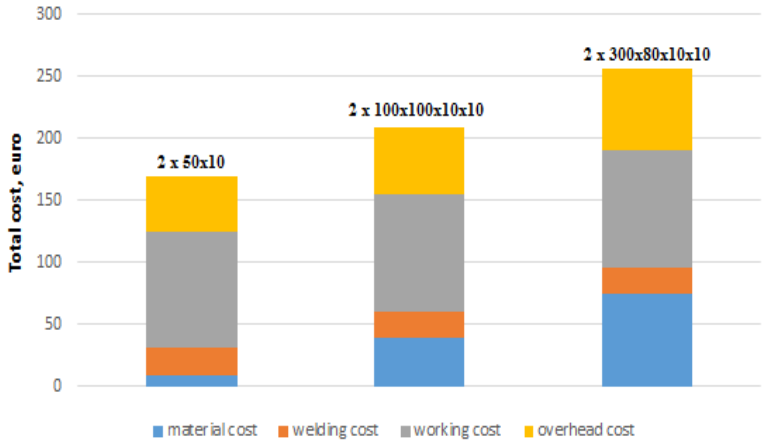

Figure 53 Subdivision of costs for retrofitting with 2 longitudinal stiffeners

It is noticeable that the solution with less material is also the cheapest one. All three scenarios present the same amount of welding costs (function of welding length). The most sensible difference is given by the cost of the material and the overhead cost (function of the total cost). Figure 54 presents the total cost in comparison to the ultimate strength ratio.

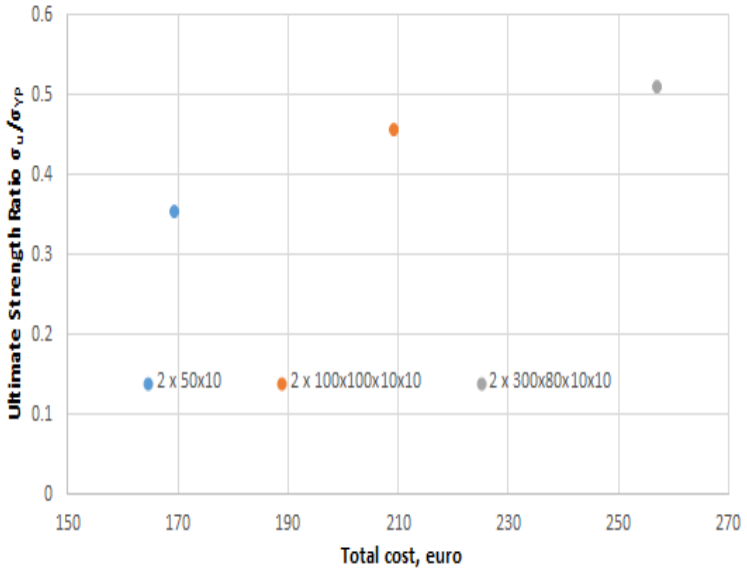

Figure 54 Total cost vs USR for retrofitting a corroded plate with opening with 2 longitudinal stiffeners

In this case, the most expensive solution is also the one that has a higher ultimate strength ratio.

7.2 CASE 2: Two longitudinal stiffeners and two transverse stiffeners

The total cost associated with the case two is presented in Figure 55.

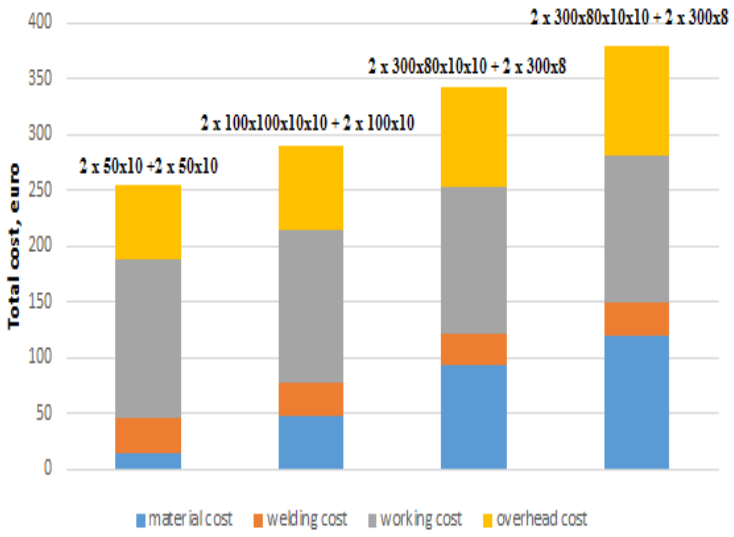

Figure 55 Subdivision of costs for retrofitting with 2 longitudinal and 2 transverse stiffeners

In this case the welding cost is different among the cases due the difference in length of the transversal elements. The material cost is directly function of the type of stiffeners. Figure 56 describes the relation between the ultimate strength ratio and the total cost for each scenario considered

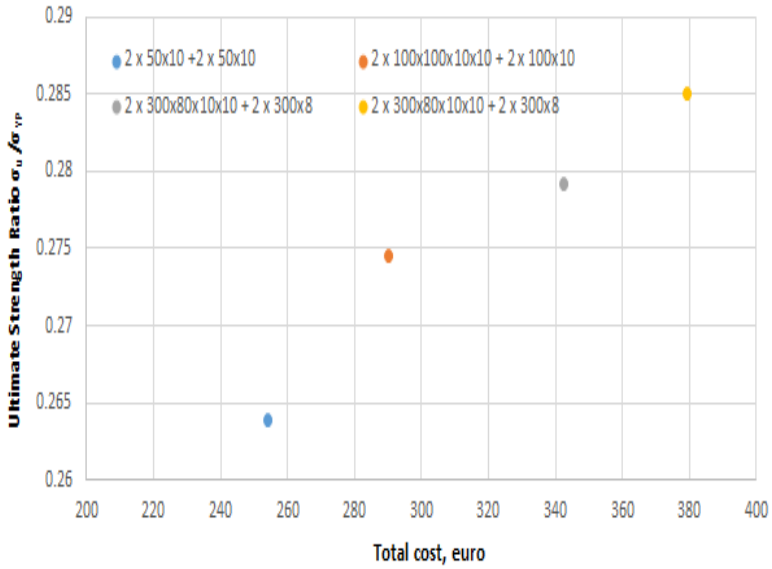

Figure 56 Total cost vs USR for retrofitting a corroded plate with opening with 2 longitudinal and 2 transverse stiffeners

As for case one, also in this the most expensive solution is the one having also the highest value of ultimate strength capacity.

7.3 CASE 3: Flange on the opening

Figure 57 shows the cost associated with the case three.

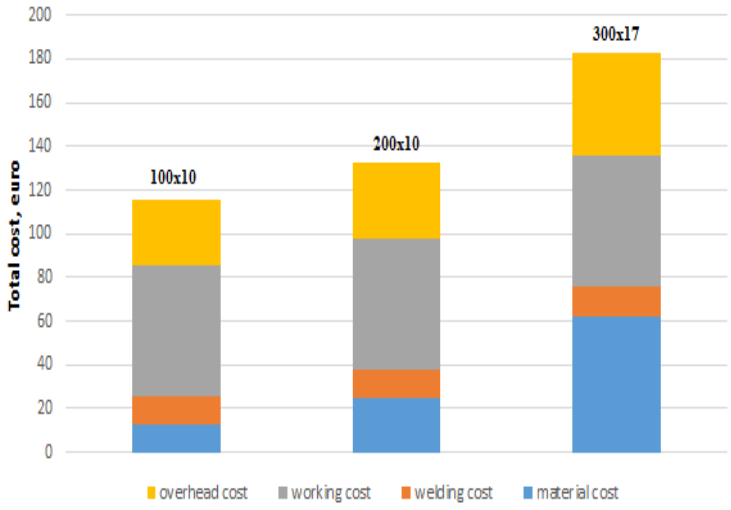

Figure 57 Subdivision of costs for retrofitting with flange on the opening

The three solutions share the same welding cost, the major difference is given by the material cost and overhead cost (function of the total cost). Figure 60 shows the relation between the total cost and the ultimate strength ratio.

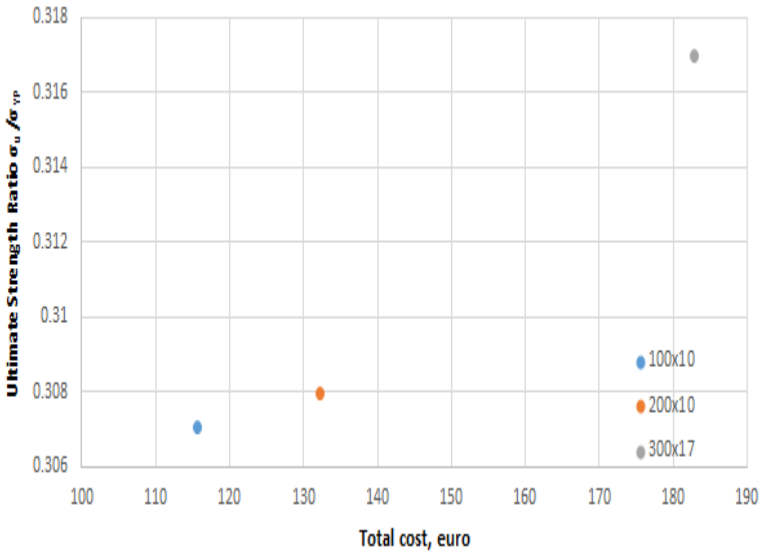

Figure 58 Total cost vs USR for retrofitting a corroded plate with opening with flange on the opening

The most expensive solution, also in this case is the one possessing the greater ultimate strength capacity.

8 Effective Thickness Assessment

An interesting comparison among all scenario studies can be done considering the effective thickness. Usually it is calculated taking into account the cross section of the model, considering the sum of the areas of the plate and the stiffeners. In this case it was decided to proceed from the total volume of the panel:

$$t_{effective} = \frac{V_{plate} + V_{stiff}}{A_{plate}} \tag{57}$$

The values resulting from the formula gives the thickness of a plane that possess the same squash load capacity of the panel with the solution adopted. It can be observed in Figure 57 the difference in effective thickness between the stiffened plate and the unstiffened plate.

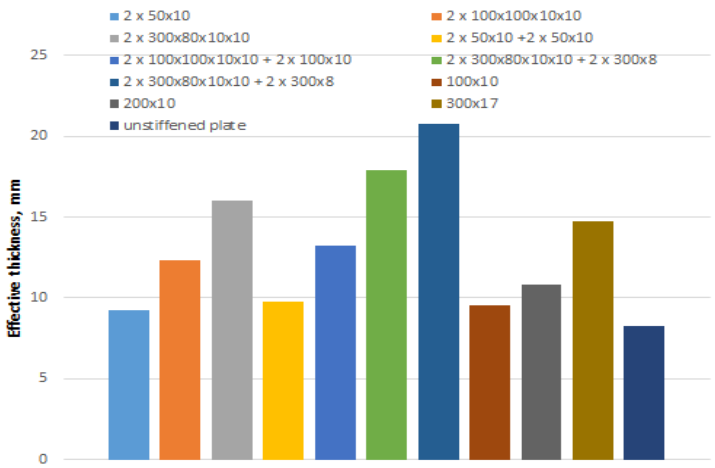

Figure 59 Comparison between effective thicknesses

It is important to remark that it was not necessary to replace a plate with a new one with bigger thickness, but this comparison denotes the efficiency and effect of different kind of reinforcement on the value of the ultimate strength in function of thickness panel. At parity of collapse capacity, a stiffened plate is thinner with a consequent saving in weight.

9 Discussion

The study has given a general idea of the possibility of retrofitting a degraded marine structure. The best solution is functional to the character that commissioned the retrofitting process. Figure 64 presents the comparison of the total cost for all the solutions adopted.

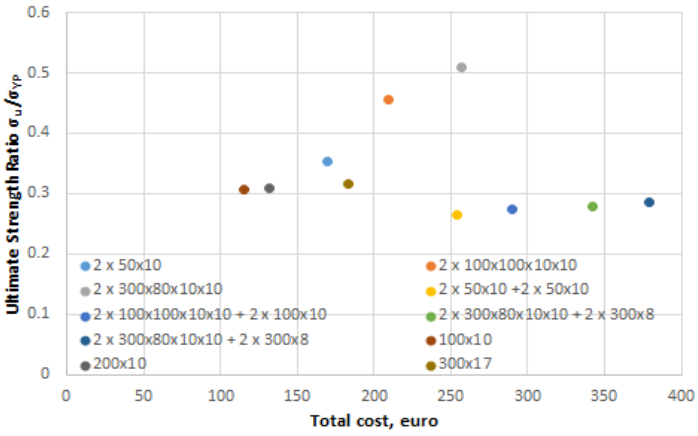

Figure 60 Total cost vs ultimate strength

It is noticeable to observe that the case with two longitudinal stiffeners give a higher value of ultimate strength with a reasonable price. On the other hand, the flange on the opening provides a collapse strength recovering similar to the original intact plate with a lower price. Connected to the economic assessment there is also the weight assessment. A high amount of mass added to the panel might be prejudiced for the cargo capacity of a ship. Figure 65 describes the comparison of the weight as a function of the ultimate strength.

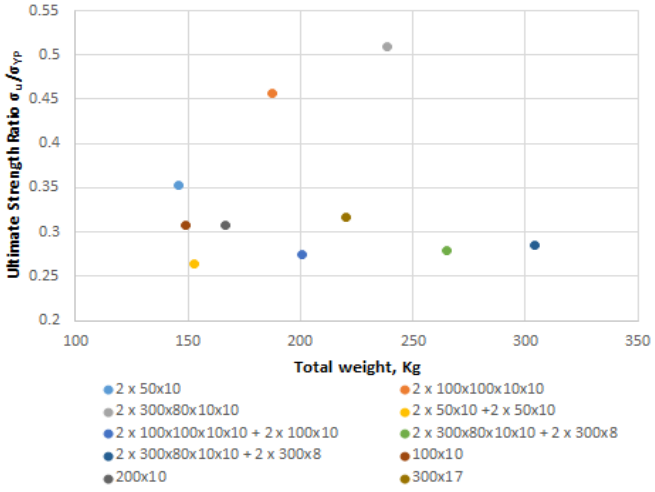

Figure 61 Total weight (plate+stiffeners) vs ultimate strength

Also in this comparison, it is noticeable to observe that the lowest weight is given by the smaller longitudinal stiffeners 50x10. This scenario also furnishes a reasonable recovering of ultimate strength. On the other hand, the grillage of two longitudinal and two transverse stiffeners provide an unfavorable solution to the retrofitting process both on weight, economical and ultimate strength recovering capacity assessments.

9.1 Final Remarks

The present study tried to accomplish the purpose to give an indication of the possibility of retrofitting of corroded marine structures. It is important to enlighten that many assumptions have been taken that could have influenced the results obtained.

The study can be classified as a conservative approach to the retrofitting process.

The finite element model possesses a considerable accuracy in the replication of the imperfection of the plate due global, local and side shifting stiffener imperfections. An improvement of those aspects might accelerate the time computing needed for each analysis. On the same level it will increase considerably the number of converged solutions.

It has to be pointed out that the arc-length method does not permit the computation of corroded plates with 0 mm of thickness. This has resulted in a high number of cases discarded of corroded plates with an excessive number of perforations.

The case scenario studied are a limited one present in the shipbuilding world. The influence of the positioning of stiffeners represents an important parameter to evaluate on the choice of different solutions. As the study briefly demonstrated, the same stiffeners placed at different locations influencing the collapse strength of the plate.

9.2 Further Work

The present study does not take into account the possibility of a programmed maintenance of the plate that might prolong it service life much more than the result presented. In addition to that, the cleaning and coating cost as well the others involved in the retrofitting/maintenance process, should be considered in their entity for a realistic prediction of service life of corroded plate.

The influence of residual stresses due to welding, the shear lag caused by the presence of stiffeners on the compression stresses acting on the plate, are worth to be investigated to enrich the present study and solve the assumption taken into account.

In particular, the welding process and the corrosion of welding material, having a different composition than the stiffener and panel, has a priority. In fact, the interest might be placed on the possibility of failure of such welding, considered perfect in the study that might cause a detachment of the stiffeners from the panel and lower sensibly the capacity of the plate.

An additional study could be the presence of pitting corrosion and cracks with an attention to the opening edge, more sensible to be highly corroded than the plate. This last concept was not taken into account in the study.

As well as retrofitting process possibility, the addition of new material different than stiffeners could be considered, as well the "patching" process, cut and replacement of part of plate with new material.

10 References

Dadrasi A. (2013) "On the Effect of Imperfection on Buckling load of Perforated RectangularSteel Plates" *Research Journal of Recent Sciences* ISSN 2277-2502 Vol. 2(3), 36-43, March (2013)

DNV-GL Rules for ClassificationDoshi K., Vhanmane S. (2014) "Ultimate Strength of Stiffened Plates Subjected to Longitudinal Compression and Lateral Pressure" OMAE2014-24637

Eurocode 3: Design of steel structures Part 1-5: Plated structural elements

Garbatov, Y., Tekgoz, M., Guedes Soares, C. (2011). "Uncertainty Assessment of the Ultimate Strength of a Stiffened Panel." Advances in Marine Structures. C. Guedes Soares, W. Fricke. London, UK, Taylor & Francis Group: 659-668

Garbatov, Y., Tekgoz, M., Guedes Soares, C. (2011). "Experimental and numerical strength assessment of stiffened plates subjected to severe non-uniform corrosion degradation and compressive load" ships and offshore structures, 2016

Garbatov, Y., Guedes Soares, C. & Wang, G. 2007. *"Nonlinear time dependent corrosion wastage of deck plates of ballast and cargo tanks of tankers."* Journal of Offshore Mechanics and Arctic Engineering-TraSsactions of the ASME, 129, 48- 55

Garbatov, Y. & Guedes Soares, C. 2010. *"Risk based maintenance of deteriorated ship structures accounting for historical data."* In: Guedes Soares, C. & Parunov, J. (eds.) Advanced ship design for pollution prevention. London, UK: Taylor & Francis Group, 131-149.

Garbatov, Y. & Guedes Soares, C. 2008. "*Corrosion wastage modelling of deteriorated bulk carrier decks".* International Shipbuilding Progress, 55, 109-125

Guedes Soares, C., (1988) "Uncertainty Modelling in Plate Buckling." Elsevier Science Publishers B.V., Amsterdam

Guedes Soares, C., Garbatov, Y., Zayed, A., Wang, G. (2008). *"Corrosion Wastage Model for Ship Crude Oil Tanks."* Corrosion Science 50(11): 3095-3106.

Guedes Soares, C., Garbatov, Y., Zayed, A., Wang, G. (2009). *"Influence of Environmental Factors on Corrosion of Ship Structures in Marine Atmosphere."* Corrosion Science 51(9): 2014-2026.

Guedes Soares, C., Gordo, J. M. (1996). *"Compressive Strength of Rectangular Plates Under Biaxial Load and Lateral Pressure."* Thin-Walled Structures 24: 231-259.

Guedes Soares, C., Gordo, J. M. (1996). *"Compressive Strength of Rectangular Plates Under Transverse Load and Lateral Pressure.*" Journal of Constructional Steel Research 36: 215-234.

Guedes Soares, C., Gordo, J. M. (1997). *"Design Methods for Stiffened Plates under Predominantly Uniaxial Compression."* Marine Structures 10: 465-497.

Guedes Soares, C., Kmiecik, M. (1993). *"Simulation of the Ultimate Compressive Strength of Unstiffened Rectangular Plates."* Marine Structures 6: 553-569.

Guedes Soares, C., Kmiecik, M. (1995). *"Influence of the Boundary Conditions on the Collapse Strength of Square Plates with Initial Imperfections."* Computational Mechanics Publications: 227-235.

Guedes Soares, C., Søreide, T. H. (1983). *"Behaviour and Design of Stiffened Plates under Predominantly Compressive Loads."* International Shipbuilding Progress 30: 13-27.

Gordo, J. M., Guedes Soares, C., Faulkner, D. (1996). *"Approximate Assessment of the Ultimate Longitudinal Strength of the Hull Girder."* Journal of Ship Research 40(1): 60-69.

Hart D, Rutherford S, Wichham A. (1986). *"Structural reliability analysis of stiffened panels."* Trans Roy Inst Naval Arch (RINA);128:293–310.

IACS, 2010. "*Common structural rules for double hull oil tankers*." International Association of Classification Societies.

Irons B, Ahmad S, 1980, *"Techniques of finite elements",* Ellis Horwood Ltd., Chichester

Ivanov, L., Rousev, S., 1979. *"Statistical estimation of reduction coefficient of ship's hull plates with initial deflections."* The Naval Architect 4, pp. 158–160.

Ivanov, L., Spencer, J., Wang, G., 2003. *"Probabilistic evaluation of hull structure renewals for aging ships",* pp. 393-406.

Johansson B., Maquoi R., Sedlacek G., Müller C., Beg D., C*ommentary and worked examples to EN 1993-1-5 "plated structural elements"*, EUR 22898 EN - 2007

Kim, U.N., Choe, I.H., Paik, J.K., 2009. *"Buckling and Ultimate Strength of Perforated Plate Panels subject to Axial Compression: Experimental and Numerical Investigations with Design Formulations."* Ships and Offshore Structures 4, pp. 337–361.

Khedmati M.R., Nouri Z., Roshanali M.M., 2012, *"A comparative computational investigation on the effects of randomly distributed general corrosion on the post-buckling behaviour of uniaxially loaded plates",* Journal of Mechanical Science and Technology 26(3)

Kumar MS, Alagusundaramoorthy P, Sundaravadivelu R. *"Ultimate strength of square plate with rectangular opening under axial compression."* J Nav Archit Mar Eng 2007; 4:15–26.

Narayanan R, Chow FY. *"Ultimate capacity of uniaxially compressed perforated plates."* Thin-Walled Struct 1984; 2:241–64.

Ok, D., Pu, Y., Incecik, A., 2007. *"Computation of ultimate strength of locally corroded unstiffened plates under uniaxial compression."* Marine Structures 20, pp. 100-114.

Paik J.K., Thayamballi A.K., 2003 "*Ultimate Limit State Design of Steel-Plated Structures"*

Paik J.K., Thayamballi A.K, Wang G., Kim B.J., 2000, *"On Advanced Buckling and Ultimate Strength Design of Ship Plating"*

Paik, J.K., Lee, J.M., Hwang, J.S., Park, Y.I., 2003c. *"A time-dependent corrosion wastage model for the structures of single-and double-hull tankers and FSOs and FPSOs."* Marine Technology 40, pp. 201-217.

Paik, J.K., 2007a. "Ultimate Strength of Perforated Steel Plates under Edge Shear Loading." Thin-Walled Structures 45, pp. 301–306.

Paik, J.K., 2007b. "Ultimate Strength of Steel Plates with a single Circular Hole under Axial Compressive Loading along Short Edges." Ships and Offshore Structures 2, *pp. 355–360.*

Qin, S., Cui, W., 2003. *"Effect of corrosion models on the time-dependent reliability of steelplated elements."* Marine Structures 16, pp. 15-34.

Saad-Eldeen S., Garbatov Y., Guedes Soares C. (2015) *"Ultimate strength assessment of steel plates with a large opening." Developments in Maritime Transportation and Exploitation of Sea Resources – Guedes Soares & López Peña (eds) 2014 Taylor & Francis Group, London, ISBN 978-1-138-00124-4*

Saad-Eldeen S., Garbatov Y., Guedes Soares C (2015) *"Experimental strength assessment of thin steel plates with a central elongated circular opening"* Journal of Constructional Steel Research 118 (2016) 135–144

Saad-Eldeen S., Garbatov Y., Guedes Soares C (2016), *"Experimental strength analysis of steel plates with a large circular opening accounting for corrosion degradation and cracks subjected to compressive load along the short edges",* Marine Structures 48 (2016) 52-67

Shanmugam, N.E., Thevendran, V., Tan, Y.H., 1999. *"Design Formula for Axially Compressed Perforated Plates." Thin-Walled Structures* 34, pp. 1–20.

Silva, J. E., Garbatov, Y. & Guedes Soares, C. 2013. *"Ultimate strength assessment of rectangular steel plates subjected to a random localized corrosion degradation."* Engineering Structures, 52, 295-305.

Singiresu S Rao, 1982, The Finite Element Method in Engineering, Elsevier India Pt. Ltd., First edition

Smith, C. S., Davidson, P. C., Chapman, J. C., Dowling, J. P. (1988). *"Strength and Stiffness of Ships' Plating under In-plane Compression and Tension."* Transactions RINA 130: 277-296.

Sun, H.H., Bay, Y., 2001. "*Time-variant reliability of FPSO hulls*." Discussion. Authors' closure. Transactions-Society of Naval Architects and Marine Engineers 109, pp. 341-366.

Tekgoz M., Garbatov Y., Guedes Soares C. (2015), *"Ultimate strength assessment of welded stiffened plates"* Engineering Structures 84 (2015) 325–339

Tekgoz M., Garbatov Y., Guedes Soares C. (2015), *"Strength analysis of ship shaped structures subjected to asymmetrical bending moment"* Analysis and Design of Marine Structures – Guedes Soares & Shenoi (Eds) 2015 Taylor & Francis Group, London, ISBN 978-1-138-02789-3

Wang, G., Sun, H., Peng, H., Uemori, R., 2009." *Buckling and Ultimate Strength of Plates with Openings*". *Ships and Offshore Structures* 4, pp. 43–53.

Wang Y., Wharton J.A., Shenoi R., 2014, *"Ultimate strength analysis of aged steel-plated structures exposed to marine corrosion damage: A review"*

Zienkiewicz O. C., Cheung Y. K., 1967, *"The Finite Element Method in Structural and Continuum Mechanics"* McGraw-Hill